Study on the mechanism of dynamic changes in the number of ciliated and non-ciliated cells in the bovine oviduct

March, 2020

Sayaka Ito

Graduate School of

Environmental and Life Science

(Doctor's Course)

OKAYAMA UNIVERSITY

Study on the mechanism of dynamic changes in the number of ciliated and non-ciliated cells in the bovine oviduct

March, 2020

Sayaka Ito

Graduate School of

Environmental and Life Science

(Doctor's Course)

OKAYAMA UNIVERSITY

CONTENTS

PREFACE

The experiments described in this dissertation were carried out at the Graduate School of Environmental and Life Science (Doctor's course), Okayama University, Japan, from April 2017 to March 2020, under the supervision of Professor Koji KIMURA.

This dissertation has not been submitted previously in whole or in part to a council, university or any other professional institution for degree, diploma or other professional qualifications.

Sayaka ITO

March, 2020

ACKNOWLEDGMENTS

I wish to my express my deep gratitude to Kiyoshi OKUDA, DVM, Ph.D., Professor emeritus of Okayama University, Okayama, Japan, and President of Obihiro University of Agriculture and Veterinary Medicine, Obihiro, Japan, and Koji KIMURA, Ph.D., Professor of Graduate School of Environmental and Life Science, Okayama, University, for his guidance, encouragement, constructive criticism, and excellent supervision and for providing me the opportunity to conduct this study. I also wish to thank Yuki YAMAMOTO, DMV, Ph.D., Assistant Professor of Okayama University, for her supports, advices, encouragement, and advice at all stages of this study. Con-focal microscopic images were obtained with the cooperation of Department of Instrumental Analysis, Advanced Science Research Center, Okayama University. It is a pleasure to express my thanks to all the members of Laboratory of Animal Reproductive Physiology for helping me during carrying out this study.

CHAPTER 1
GENERAL INTRODUCTION

Oviductal physiology in reproductive events

The first anatomical description of a mammalian oviduct was published by Fallopius in 1561 [1]. The oviduct is the tubular organ connecting the ovary and uterus [2], and it plays an essential role in the establishment of pregnancy by providing an optimal micro-environment for the fertilization and development of the embryo [3]. The oviduct is divided into the following three regions: fimbriae, ampulla, and isthmus [4,5]. The fimbriae, which is the distal entrance of the oviduct, capture the oocyte after ovulation, the ampulla is the site where fertilization takes place, and the isthmus serves as a sperm reservoir [6]. Each oviductal region has various specific functions. The epithelium of the ampulla has greater number of folds than the isthmus, and transports the ovulated oocyte to the site of fertilization by oviductal fluid flow which is produced by ciliary beating and smooth muscle motility. The isthmus has a more muscular wall than ampulla, and transports embryos to the uterus by peristaltic contractions of smooth muscle. After fertilization, appropriate timing of the transport is the essential for the embryo to obtain the capacity of implantation [7,8]. The necessity of ciliary beating in successful pregnancy is explained by the fact that the decrease of ciliary beating reduces fertility in women with immotile cilia syndrome [9]. Various hormonal factors have been shown to modulated the ciliary beating in the oviduct. Several studies have reported that the ovarian steroids and other factors produced by the oviduct, such as PGE2, PGF2α, and adrenomedurin regulate ciliary beat frequency in the oviduct [10-15]. Thus, the regulation mechanisms of transport in the oviduct by ciliary beating has been clarified.

Several studies have documented infertility due to oviductal disorders [9,16,17].

Ciliary beating and smooth muscle contraction are important functions in the oviduct for transport of the embryo from the oviduct toward the uterus, and their defects may contribute to ectopic pregnancy [18]. The ectopic pregnancy occurs outside of the uterine cavity, and over 98% of ectopic pregnancy represents implantation of embryo in the oviduct, known as tubal ectopic pregnancy (tEP) [19,20]. The aetiology of ectopic pregnancy is unclear [18,21], however, recent studies implied that several factors regulating ciliary beating are deficient in woman with tEP [16,18], and cigarette smoking and infections significantly increases the risk of tEP [22,23,21].

In addition to the above, the ciliary dysfunction in the oviduct may also cause ectopic pregnancy or infertility in women. Primary ciliary dyskinesia (PCD) is an autosomal recessive disorder of motile cilia that are associated with impaired ciliary motion [24,25]. Motile cilia fulfil crucial and diverse functions in the different organs [26]. For example, ciliary beating in the airway enables to clearance from inhaled particles and virus [27], ependymal cilia in the brain contribute to drive polarized fluid flow important for cerebrospinal fluid propulsion [28], and in oviduct, ciliated cells are needed for successful embryo transport toward the uterus [29]. In PCD, dysfunction of oviductal cilia results in increase of subfertility and tEP [30]. Vasquez et al. demonstrated that woman with tEP showed reduction in the number of ciliated cells in comparison with normal pregnant woman [17]. Furthermore, recent studies suggest that disruption of ciliogenesis at cellular level can lead to embryo transport defects [29,31].

Morphological changes in the bovine oviduct

The oviductal epithelium is composed of two types of cells, ciliated and non-ciliated cells [32]. In mammalian oviduct, non-ciliated cells produce oviductal fluid

containing rich in amino acids and various molecules that provide an optimal micro-environment for sperm capacitation, fertilization, embryonic survival and development [2,33], and ciliated cells play a role in embryo and oocyte transport by means of ciliary beating [32]. The percentage of ciliated cells dramatically increases from the isthmus to the fimbriae. In cattle, the proportion of ciliated cells in the oviductal lumen is abundant at the follicular phase, whereas the proportion of secretory cells gradually increases with formation of the corpus luteum [34]. The mechanisms underlying these changes in the proportions of ciliated and non-ciliated cells are poorly understood.

Aim of the present study

At first, cyclic changes in the proportion of proliferating and apoptotic cells was investigated to clarify the remodeling mechanisms in the bovine oviductal epithelium. Secondly, to clarify ciliogenesis process from non-ciliated cells into ciliated cells, we examined expression pattern of ciliogenesis associated factors in the bovine oviductal epithelial cells *in vivo* compared with the *in vitro* state and during cell culture.

CHAPTER 2
Regulation od oviductal function by proliferation and apoptosis of oviductal epithelial cells in cattle

INTRODUCTION

Two types of oviductal epithelial cells, non-ciliated and ciliated, play crucial roles in the first days of pregnancy [2,33]. Non-ciliated cells produce oviductal fluid that is rich in amino acids and various molecules that are required for an optimal micro-environment for embryo survival and development [33]. Beating of motile cilia produces a stream of oviductal fluid, which transports an ovulated cumulus-oocyte complex to the ampulla of the oviduct where fertilization occurs [32]. The stream also transports the embryo to the uterus [35]. Since the proportions of these two cell types change during the estrous cycle [34], oviductal epithelial functions are possible to depend on epithelial morphological changes. In the present study, we hypothesized that cyclic cell mitosis and apoptosis contribute to changes of the proportion of ciliated and non-ciliated epithelial cells in the bovine oviduct during the estrous cycle.

To test this hypothesis, we 1) immunohistochemically investigated changes in the proportions of cells positive for Ki67 (proliferation marker), cleaved caspase-3 (CCP3; apoptotic cellular marker), and FOXJ1 (ciliated cell marker) in the bovine oviductal epithelium during estrous cycle and 2) determined the localizations of Ki67 and FOXJ1 or PAX8 (non-ciliated cell marker) by double immunofluorescent staining to clarify which types of epithelial cells undergo proliferation.

MATERIAL AND METHODS

Collection of bovine oviduct tissues

Cow oviducts were collected at a local abattoir within 10-20 min after the exsanguination. The stages of the estrous cycle were determined based on a macroscopic observation of the ovary and the uterus [36,37]. Oviductal tissues were collected from cows at six different stages of the estrous cycle (Day 0; day of ovulation, Days 2-3, Days 5-6, Days 8-12, Days 15-17 and Days 19-21). The ampullary and isthmic sections of the oviducts being ipsilateral to the corpus luteum or the dominant follicle, were formalin-fixed and paraffin-embedded.

Immunohistochemistry

Oviductal sections of the ampulla and isthmus were sliced at 6 μm thickness. Antigen retrieval was performed by microwaved in 0.1 M Tris-EDTA buffer (pH 9.0) for 15 min at 600 W. Endogenous peroxidase activity was quenched in distilled water with 0.3% H_2O_2 for 30 min. Nonspecific binding was blocked at room temperature for 20 min in normal horse serum (MP-7500; Vector Laboratories Inc, Burlingame, CA, USA). The sections were incubated with anti-FOXJ1 rabbit polyclonal antibody (HPA005714; Sigma-Aldrich, St. Louis, MO, USA; dilution 1:200), anti-cleaved caspase-3 (CCP3) rabbit antibody (#9661; Cell signaling, dilution 1:100) or anti-Ki67 mouse monoclonal antibody (M7240; Dako-Cytomation, Glostrup, Denmark; dilution 1:200) overnight at 4°C. After incubation, the sections were washed with PBS 3 times, and incubated with ImmPRESS UNIVERSAL reagent, anti-mouse/rabbit Ig (MP-7500; Vector Laboratories Inc) for 30 min according to the manufacture's instruction. The sections were visualized

with 0.05% 3,3-diaminobenzezidine tetrahydrochloride (DAB), containing 0.01% H_2O_2 (pH 7.6, 0.05 M Tris-HCl buffer solution, 047-27011; Wako Pure Chemical Industries, Osaka, Japan), and counterstained with hematoxylin (4302; MERCK Darmstadt, Germany) and examined at x500 magnification to calculate the proportion of $Ki67^+$, $CCP3^+$, and $FOXJ1^+$ cells.

Each cell number was counted by the "point count method" as described previously [36,38,39]. Briefly, the sections were covered with a 29 x 39 grid (1131 cross-points). Two persons who were blind to stages of estrous cycle counted the number of cells that were positive or negative for Ki67, CCP3, and FOXJ1 at cross-points in randomly chosen areas on each section. Positively-stain cells were stained with both DAB and hematoxylin and negatively-stained cells were stained only with hematoxylin. The counts of the two persons were averaged. The proportions of the $Ki67^+$, $CCP3^+$, and $FOXJ1^+$ epithelial cells were calculated as X/Y x100, where X was the total number of positive epithelial cells and Y was the total number of epithelial cells.

Immunofluorescence

Co-localization of FOXJ1 and Ki67 in the oviductal epithelium

The ampullary and isthmic sections on Days 19-21 were incubated with both FOXJ1 and Ki67 antibodies overnight at 4°C, washed with PBS 3 times, incubated with both goat anti-rabbit IgG antibody conjugated with Alexa Fluor 488 (A11008; Life Technologies, Carlsbad, CA, USA) and goat anti-mouse IgG antibody conjugated with Alexa Fluor 594 (A11005; Life Technologies) for 60 min at room temperature, and covered with ProLong Gold Antifade Reagent with DAPI (P36935; Life Technologies).

Co-localization of PAX8 and Ki67 in the oviductal epithelium

The ampullary and isthmic sections on Days 19-21 were incubated with both anti-PAX8 mouse monoclonal antibody (ACR438A; BIOCARE Medical LLC, Concord, MA, USA; dilution 1:100) and anti-Ki67 rabbit monoclonal antibody (ACR325A; BIOCARE Medical LLC; dilution 1:200) antibodies overnight at 4°C, washed with PBS 3 times, incubated with both goat anti-mouse IgG antibody conjugated with Alexa Fluor 594 and goat anti-rabbit IgG antibody conjugated with Alexa Fluor 488 for 60 min at room temperature, and covered with ProLong Gold Antifade Reagent with DAPI.

Statistical analysis

All experimental data are shown as the mean ± SEM. The statistical significance of differences was assessed by analysis of variance (ANOVA) followed by Tukey's multiple comparison test using GraphPad Prism version. 6.03 (GraphPad Software, La Jolla, CA, USA). *P* values less than 0.05 were considered to be statistically significant.

RESULTS

Ki67-positive cells

Ki67$^+$ cells in the ampulla were most abundant on Days 19-21 (follicular stage) and Day 0 (the day of ovulation) and least abundant on Days 8-12 and Days 15-17 (Fig. 1a-c, g), while in the isthmus, they were most abundant on Day 0 and Days 19-21, and undetectable on Days 8-12 (Fig. 1d-g).

CCP3-positive cells

Cleaved-caspase-3$^+$ cells in the bovine oviduct were detected in both the ampulla and isthmus during the estrous cycle. The proportion of CCP3$^+$ cells was highest on Days 8-12 in the ampulla (Fig. 2a-c, g), while in the isthmus, it was most abundant at the time of ovulation (Fig. 2d-g).

FOXJ1-positive (ciliated) cells

The proportion of FOXJ1$^+$ cells in the ampulla was highest on Day 0, and lowest on Days 8-12 (Fig. 3a-c, g), while in the isthmus, it did not significantly change during the estrous cycle (Fig. 3d-g).

Co-localization of Ki67 and FOXJ1 or PAX8

On Days 19-21, all the Ki67$^+$ cells were FOXJ1-negative (were not ciliated) in both the ampulla and isthmus (Fig. 4a-f). All the Ki67$^+$ cells were PAX8 positive in both the ampulla and isthmus (Fig. 4g-l).

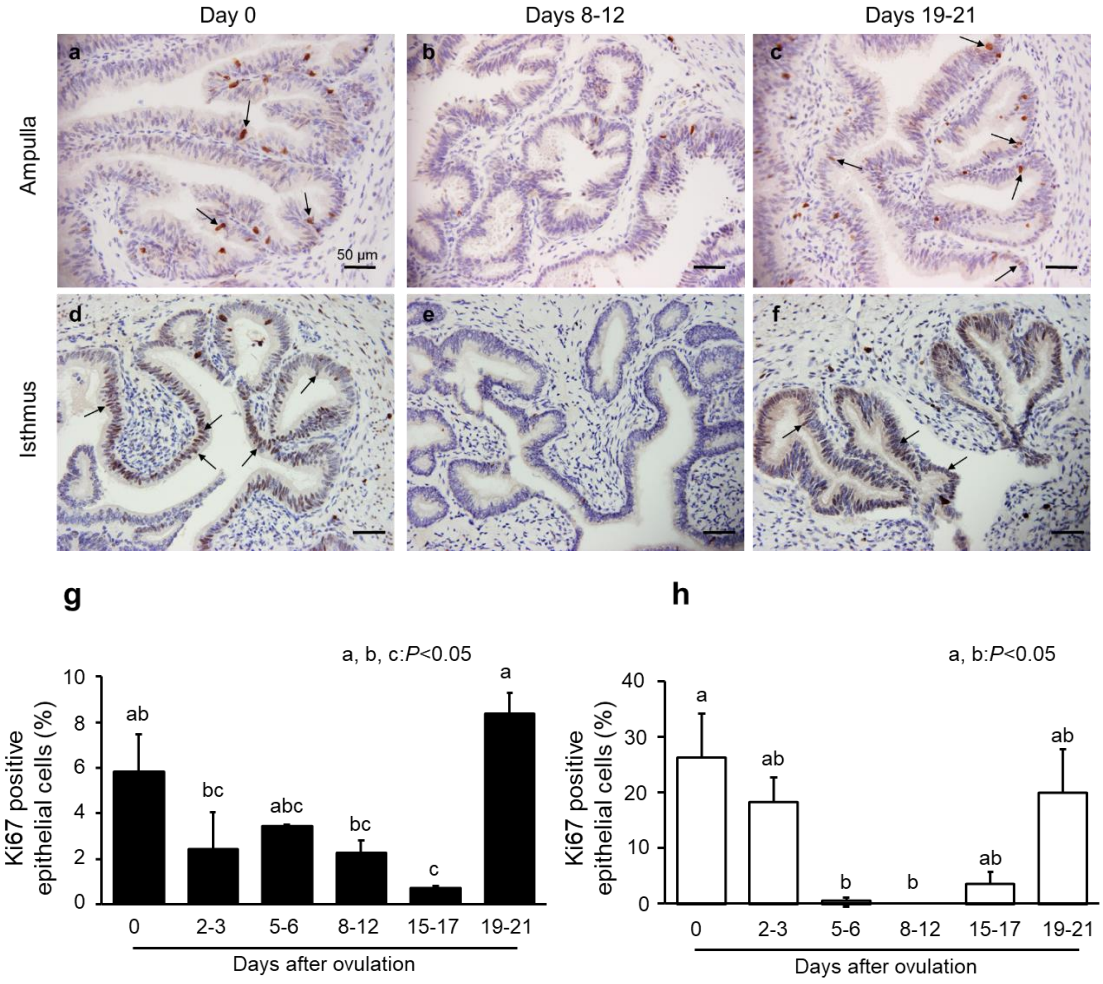

Fig.1

Immunohistochemical localization of cells showing positive nuclear staining for Ki67 (arrow) in the (**a-c**) ampulla and (**d-f**) isthmus of the bovine oviduct during the estrous cycle (**a, d** Day 0; **b, e** Days 8-12; **c, f** Days 19-21). Scale bars represent 50 μm. Percentages of $Ki67^+$ epithelial cells in the (**g**) ampulla (black bar) and (**h**) isthmus (white bar) of the bovine oviduct during the estrous cycle (mean ± SEM, n = 3 experiments). Percentages were derived from dividing the number of positively stained epithelial cells by the total number of epithelial cells under 1131 cross-points in each histological section at ×500 magnification. Different superscript letters indicate significant differences ($P < 0.05$).

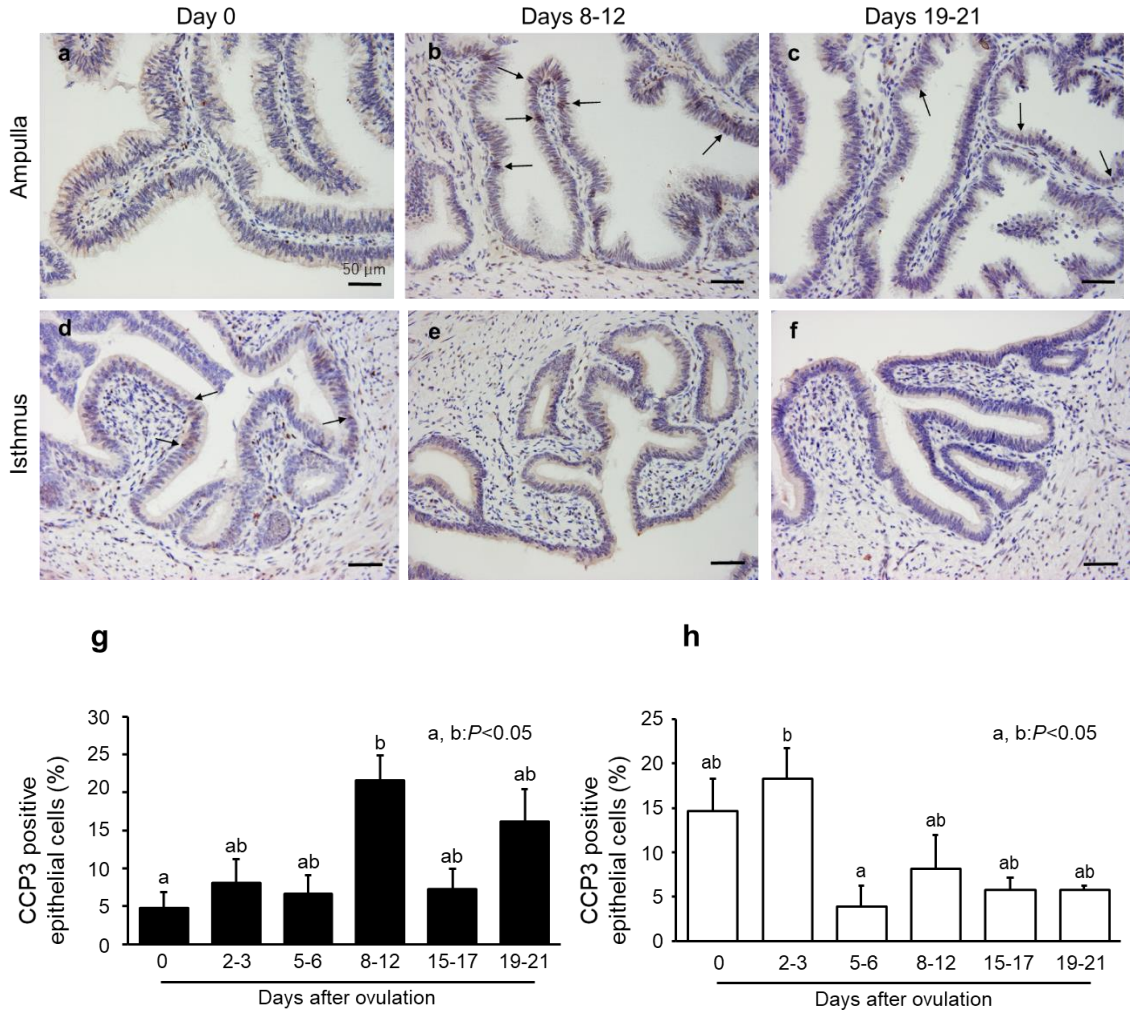

Fig. 2

Immunohistochemical localization of cells showing positive staining for cleaved caspase-3 arrow in the (**a-c**) ampulla and (**d-f**) isthmus of the bovine oviduct during the estrous cycle (**a, d** Day 0; **b, e** Days 8-12; **c, f** Days 19-21). Scale bars represent 50 µm. Percentages of cleaved caspase-3^{+} epithelial cells in the (**a**) ampulla (black bar) and (**h**) isthmus (white bar) of the bovine oviduct during the estrous cycle (mean ± SEM, n = 3 experiments). Percentages were derived from dividing the number of positively stained epithelial cells by total number of epithelial cells under 1131 cross points in each histological section at ×500 magnification. Different superscript letters indicate significant differences ($P < 0.05$).

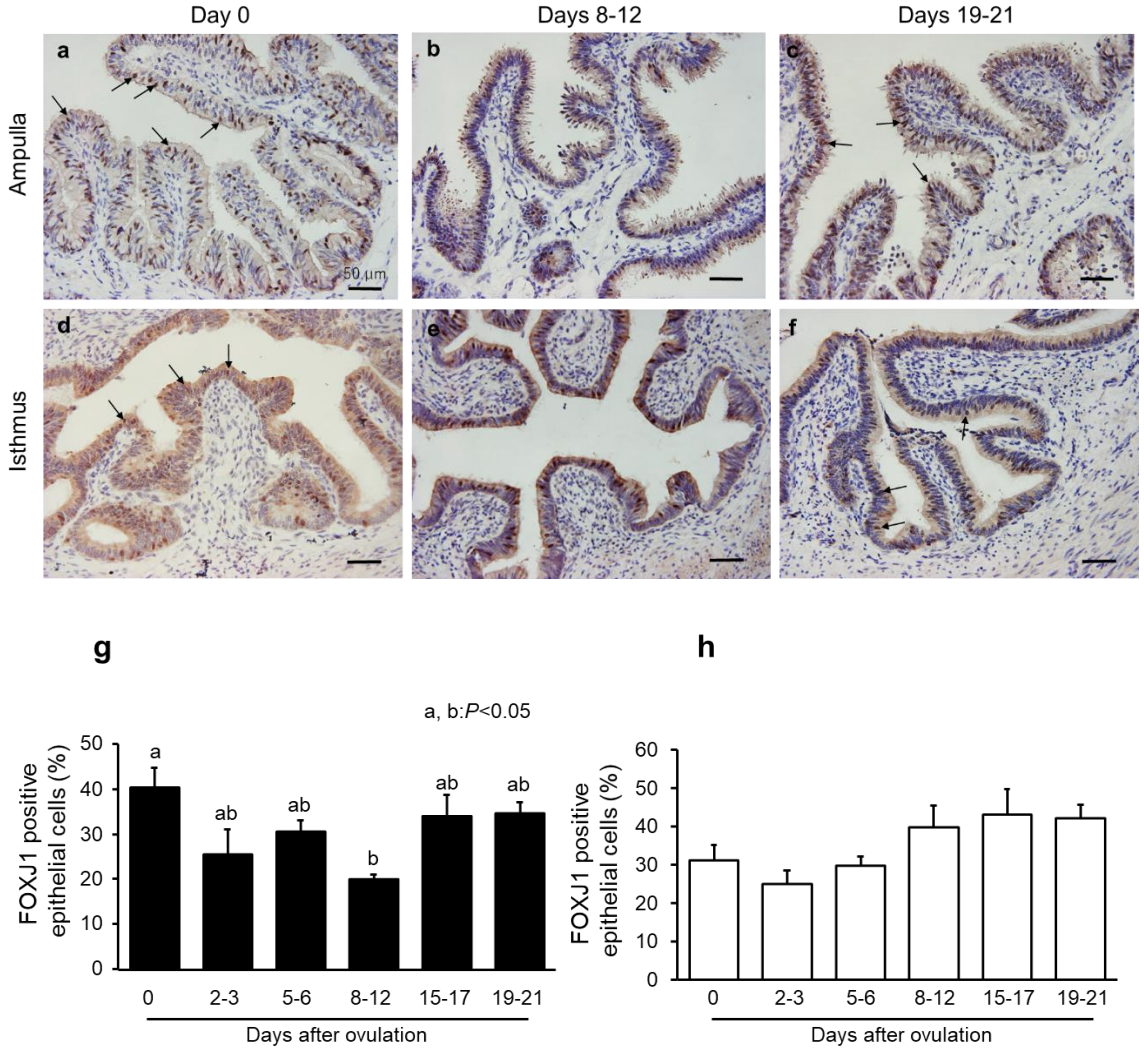

Fig. 3

Immunohistochemical localization of cells showing positive nuclear staining for FOXJ1 (arrow) in the (**a-c**) ampulla and (**d-f**) isthmus of the bovine oviduct during the estrous cycle (**a, d** Day 0; **b, e** Days 8-12; **c, f** Days 19-21). Scale bars 50 µm. Percentages of $FOXJ1^+$ epithelial cells in the (**g**) ampulla (black bar) and (**h**) isthmus (white bar) of the bovine oviduct during the estrous cycle (mean ± SEM, n = 3 experiments). Percentages were derived from dividing the number of positively stained epithelial cells by the total number of epithelial cells under 1131 cross-points in each histological section at ×500 magnification. Different superscript letters indicate significant differences ($P < 0.05$).

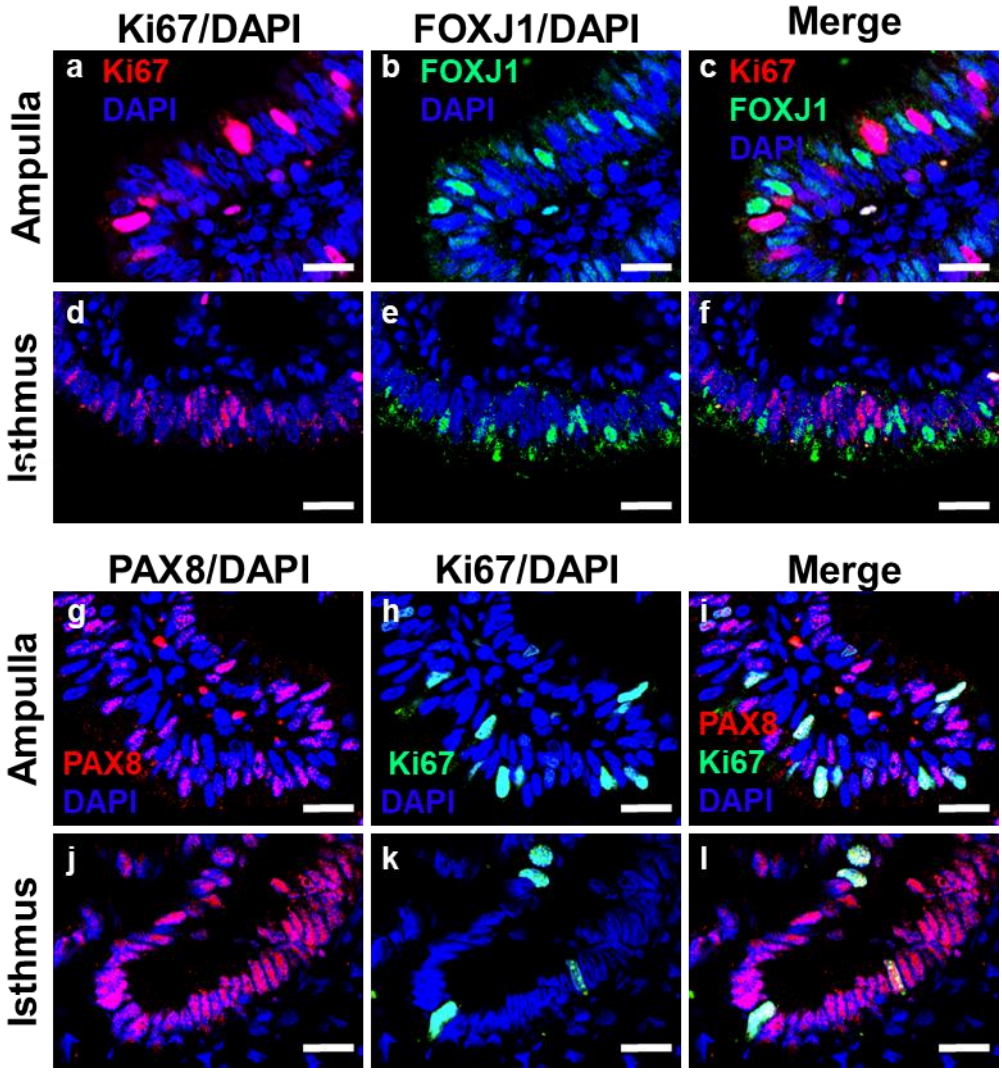

Fig. 4

(a–f) Distributions of cells showing positive nuclear staining for Ki67 (red Alexa 594) and positive ciliary nuclear for FOXJ1 (green Alexa 488) in the ampulla and isthmus of the bovine oviduct. Cell nuclei were counterstained with DAPI (blue). (**g–l)** Distributions of cells showing positive nuclear staining for Ki67 (green Alexa 488) and positive non-ciliated nuclear for PAX8 (red Alexa 594) in the ampulla and isthmus of the bovine oviduct. Cell nuclei were counter-stained with DAPI (blue). Scale bars 20 µm.

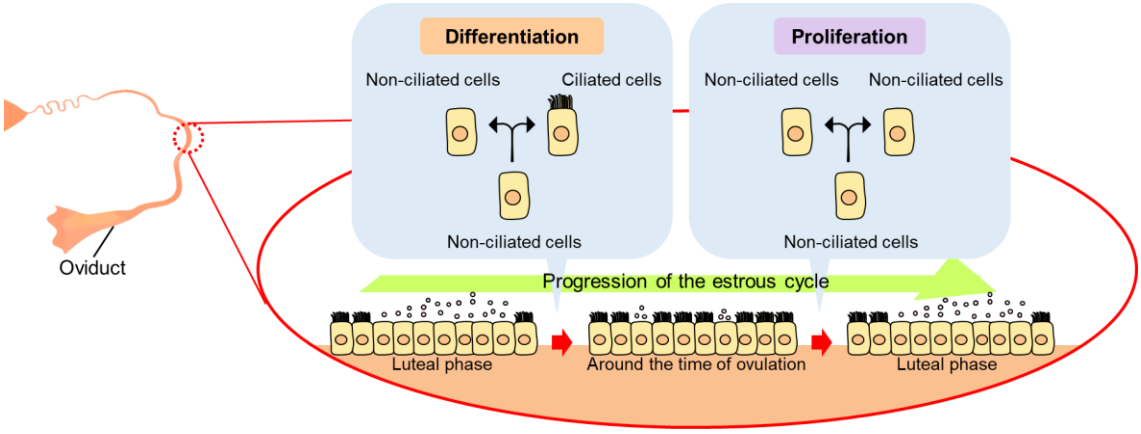

Fig. 5

Diagram of the hypothesis about the change of proportions of ciliated and non-ciliated cells in the bovine oviductal epithelium. The proportion of ciliated cells increases toward ovulation, in contrast that of non-ciliated cells gradually increase with progression of luteal formation. These dramatic changes of the epithelium may be regulated by differentiation and proliferation of non-ciliated cells.

DISCUSSION

In the present study, we showed that the proportions of two types of oviductal epithelial cells, non-ciliated and ciliated, change during estrous cycle. The proportion of ciliated cells in the ampulla was highest around the time of ovulation (Fig. 1h), although that in the isthmus was not changed throughout the estrous cycle in bovine oviduct (Fig. 2h). These findings are supported by the previous report that the proportion of ciliated cells increased in the ampulla at the follicular phase, but not in the isthmus in cattle [34]. The early embryo is transported by motility of the myosalpinx in the isthmus, whereas the transport of the cumulus-oocyte complex (COC) through the ampulla depends on ciliary beating [3,2]. Since ciliated cells produce the stream of oviductal fluid to transport COC toward the site of fertilization [2], the increase of the proportion of ciliated cells may support the COC transport by producing the optimal stream of oviductal fluid.

Epithelial tissue is constantly replaced by cell proliferation [40]. Oviductal epithelium undergoes cyclic changes during the estrous cycle [34]. In the present study, we detected $Ki67^{+}$ cells in the epithelium of ampulla and isthmus, and showed that oviductal epithelial cells proliferate around the time of ovulation. These results suggest that oviductal epithelium is remodeled by the proliferation, and it is associated with estrous cycle. The turnover of epithelial cells is rapid in the proximal lung, and slower in the more distal regions [41,42]. The present study also showed that the proportion of $Ki67^{+}$ cells in the isthmus is higher than the ampulla, suggesting that the rate of cell turnover is dependent on the region of the oviduct.

Ovarian steroids, estradiol-17β (E2) and progesterone, are important modulators of physiology of the bovine oviduct. We found that the proportion of $Ki67^{+}$ cells in the oviductal epithelium is the highest around the time of ovulation, as previously reported

in the porcine, human, and bitch oviduct [43-46]. It is thought that this high proliferative activity is regulated by E2 in the oviduct[46,32]. Given that the concentration of E2 in the bovine oviduct is highest before ovulation [47], and follicular fluid containing high concentration of E2 enters into the oviduct with COC at ovulation [48], proliferation of the bovine oviductal epithelial cells might also be promoted by E2.

Expressions of Ki67 in porcine and canine oviductal epithelia were observed under conditions of high levels of E2, while apoptotic cells were observed during the luteal phase [44]. In addition, expressions of caspases which induce apoptosis have been reported to be increased at diestrus in the murine oviduct [49]. Apoptosis to remove unwanted or *chlamydia* infected cells plays an important role in the maintenance of homeostasis and normal functions in oviductal tissues [50-52]. In the present study, we detected cleaved-caspase-3^{+} cells in the bovine oviduct during the estrous cycle. (Fig 2), suggesting that apoptosis in the bovine oviductal epithelium is active. The epithelial cells are constantly turning over by proliferation and death [53]. To maintain the proper function of epithelia, the number of cells need to be properly controlled [54]. Since we also detected cleaved-caspase-3 protein in the bovine oviduct (Fig. 2), caspase cascades followed by apoptosis may also contribute to the remodeling of oviductal epithelium. Further studies are needed to clarify the roles of apoptotic in the regulation of oviductal epithelial remodeling.

FOXJ1 and PAX8 are commonly used as markers of ciliated and non-ciliated cells, respectively [55,56]. Interestingly, the cyclic changes of proportion of $FOXJ1^{+}$ cells (ciliated cells) were coincident with that of $Ki67^{+}$ cells. Moreover, all the $Ki67^{+}$ cells were FOXJ1 negative (non-ciliated cells) in both the ampulla and isthmus. In addition, all the $Ki67^{+}$ cells were $PAX8^{+}$, showing that only non-ciliated cells enter the cell cycle and

proceed proliferation. Those findings suggest that parent non-ciliated cells give rise to both daughter non-ciliated cells and ciliated cells by proliferation and differentiation, respectively. Recently, tracheal non-ciliated cells were shown to differentiate into ciliated cells in mice [57]. Our findings imply that ciliated cells in the oviduct are also given rise from non-ciliated cells. Although the detailed mechanism has not been manifested in the present study.

In conclusion, the present results show that both cell proliferation and apoptosis are active in the bovine oviductal epithelium, and that the proportions of ciliated and non-ciliated cells change during the estrous cycle. Moreover, we demonstrated that only $PAX8^+$ cells (non-ciliated cells) proliferate. These results suggest that remodeling of bovine oviductal epithelium is regulated by differentiation and/or proliferation of non-ciliated cells, and that the oviductal epithelium remodeling provides the optimal environment for gamete transport, fertilization and embryonic development.

SUMMARY

Oviductal epithelium undergoes dramatic morphological and functional changes during the estrous cycle. In cattle, the proportion of ciliated cells is abundant at the follicular phase, whereas the proportion of non-ciliated cells is abundant at the luteal phase. However, the mechanisms of this change in the oviductal epithelium during the estrous cycle remain unclear. Here, we investigated cyclic cell proliferation and apoptosis contribute to the remodeling of oviductal epithelium during the estrous cycle. The proportion of $Ki67^+$ cells was highest at the day of ovulation (Day 0) and Days 19-21, whereas that of $CCP3^+$ cells was highest on Days 8-12 in the ampulla. By contrast, the proportions of both $Ki67^+$ and $CCP3^+$ cells were highest on Day 0 and Days 2-3, and $Ki67^+$ cells were not observed on Days 8-12 in the isthmus. In the ampulla, the proportion of $FOXJ1^+$ cells was highest on Day 0 and decreased on Days 8-12 by 50%, while in the isthmus it did not change during the estrous cycle. All the $Ki67^+$ cells were $PAX8^+$ and $FOXJ1^-$ in both the ampulla and isthmus. The overall findings suggest that epithelial remodeling, which is regulated by differentiation and/or proliferation of non-ciliated cells of the oviduct, provides the optimal environment for gamete transport, fertilization and embryonic development.

CHAPTER 3

Analysis of ciliogenesis process in the bovine oviduct based on immunohistochemical classification

INTRODUCTION

The oviductal epithelium is composed of ciliated and non-ciliated cells [32]. The proportions of these cells change during the estrous cycle [34]. However, the mechanism underlying this cyclic change in the cell proportions remains unclear. The results of chapter 2 showed that in spite of none of the FOXJ1+ cells (ciliated cells) proliferating, the proportion of FOXJ1+ cells dramatically change during the estrous cycle implied that ciliated cells are derived from non-ciliated cells. In chapter 2, since we examined the change in the proportion of the cells, an increase or decrease in the cell number has not been elucidated from the change in the proportion. Therefore, in this chapter, we investigated the change in the number of cells during the estrous cycle.

Several proteins are expressed in a cell type in a specific manner in the bovine oviduct. Acetylated-α-tubulin is a marker of the ciliary axoneme in cilia [58,59]. PAX8 is commonly used as a marker of non-ciliated cells [60,61]. FOXJ1 and MYB are required for motile ciliogenesis [62,63]. Ki67 is a cellular marker of proliferation [64]. Recently, we demonstrated that none of the ciliated cells ($FOXJ1^+$ cells) co-expressed Ki67 [65], indicating that non-ciliated cells are able to give rise to ciliated cells.

Similar to the epithelial cells in the oviduct, the epithelial cells in the airway are composed of secretory (non-ciliated) cells and ciliated cells [66,67,26]. There are multiple distinct cell types in the airway, and the regulation of airway epithelial cell differentiation is complex. It is thought that the ciliated cells in the airway are terminally differentiated cells, and further, that they are derived from non-ciliated cells [68,69]. The non-ciliated

cells lining the airway can be classified into four types of cells, namely basal cells, Clara (secretory) cells, goblet cells, and neuroendocrine cells [70]. Basal cells give rise to both ciliated and Clara cells [71,68]. Clara cells and neuroendocrine cells are also capable of differentiation into ciliated cells [72,73]. Since the structure of the oviduct is similar to that of the trachea, it is possible that the same differentiation system may exist in the oviduct. However, the different types of non-ciliated cells in the bovine oviduct have not previously been elucidated.

Thus, the objective of our study was to clarify the different cell types in the bovine oviductal epithelium and to investigate ciliogenesis from non-ciliated cells into ciliated cells.

MATERIAL AND METHODS

Collection of bovine oviduct tissues

The bovine oviducts were collected from a local abattoir within 10–20 min after the exsanguination. A careful examination was performed so that any infected ovaries or uteri could be omitted from the experiment. The different stages of the estrous cycle were determined based on the macroscopic observation of the ovary and the uterus [74,37,36]. In brief, during Stage I the ovary contains a newly formed corpus luteum (CL) with a diameter of 0.5–1.5cm. The Stage II CL is characterized by being fully formed (the diameter of the CL is 1.6–2.0 cm). Stage III begins when the red or brown color disappears, and the internal appearance of the entire CL is orange. During Stage IV, the ovary contains a large follicle and a regressed CL. The ampullary oviductal tissues were collected from cows at four different stages of the estrous cycle (Stage I, Days 1–4; Stage II, Days 5–10; Stage III, Days 11–17; Stage IV, Days 18–20). The ampullary sections of those oviducts that were ipsilateral to the CL or the dominant follicle were fixed in 4% paraformaldehyde and then embedded in paraffin.

Immunohistochemistry and cell counting

The bovine oviductal sections of the ampulla (n = 8 per stage, unless otherwise indicated) were sliced to a 4–μm thickness, microwaved in 0.1 M Tris-EDTA buffer (pH 9.0) for 15 min at 600 W to prepare the antigen, incubated in 5% bovine serum albumin-PBS for 1 h at room temperature to block non-specific binding, and then incubated with the relevant primary antibody overnight at 4°C in a hydrated chamber. The following primary antibodies were used in this study: rabbit anti-acetylated-α-tubulin (1:500, ab179484,

Abcam, Cambridge, UK), rabbit anti-FOXJ1 (1:00, AMAb91255, Sigma Aldrich, St Louis, MO, USA), mouse anti-FOXJ1 (1:100, HPA005714, Sigma Aldrich), rabbit anti-PAX8 (1:100, ACR438, Biocare Medical, Concord, MA, USA), mouse anti-PAX8 (1:100, GTX101583, GeneTex, Los Angeles, CA, USA), mouse anti-Ki67 (1:200, M7240, Dako-Cytomation, Glostrup, Denmark), rabbit anti-Ki67 (1:200, ACR325A, Biocare Medical), and mouse anti-MYB (1:100, sc-74512, Santa Cruz, Santa Cruz, CA, USA). The mouse anti-PAX8 (GTX101583) was used for the double staining experiment with FOXJ1, while the mouse anti-Ki67 (M720) and mouse anti-FOXJ1 (HPA005714) were used for the double staining experiment with acetylated-α-tubulin. The sections were washed three times in PBS for 5 min, incubated with goat anti-rabbit IgG antibody conjugated with Alexa Fluor 488 (1:500; A11008, Life Technologies, Carlsbad, CA) and goat anti-mouse IgG antibody conjugated with Alexa Fluor 594 (1:500, A11005, Life Technologies) for 60 min at room temperature, and then covered with ProLong Gold Antifade Reagent with DAPI (P36935, Life Technologies). The sections were mounted on an Olympus FSX100 (Olympus) and observed under the 200X objective or higher. Each digital picture was captured as a TIF file. A length of approximately 1 mm of the epithelium was measured along the basal membrane, and the total number of positive and negative epithelial cells located above the 1-mm basement membrane were counted on the screen (more than 380 total epithelial cells) in three frames for each section in each immunohistochemical analysis.

Double staining experiments

To classify the oviductal epithelial cells based on histological and immunological morphology, we performed double immunostaining experiments with either acetylated-

α-tubulin and FOXJ1 or PAX8 and FOXJ1. Moreover, to clarify which types of cells undergo mitosis, we performed double immunostaining experiment with acetylated-α-tubulin and Ki67. The ampullary sections were incubated with both FOXJ1 and acetylated-α-tubulin or with PAX8 acetylated-α-tubulin and Ki67 antibodies overnight at 4°C, washed three times with PBS, incubated with both goat anti-rabbit IgG antibody conjugated with Alexa Fluor 488 and goat anti-mouse IgG antibody conjugated with Alexa Fluor 594 for 60 min at room temperature, and then covered with ProLong Gold Antifade Reagent with DAPI.

Investigation of the MYB-positive cells

To identify the presence of MYB^+ cells in the bovine oviductal epithelium, we examined the co-localization of MYB and FOXJ1 or PAX8. Moreover, to investigate whether the MYB^+ cells could undergo mitosis, the co-localization of MYB and Ki67 was examined. The ampullary sections were incubated with both MYB and FOXJ1, PAX8, or Ki67 antibodies overnight at 4°C, washed three times with PBS, incubated with both goat anti-rabbit IgG antibody conjugated with Alexa Fluor 488 and goat anti-mouse IgG antibody conjugated with Alexa Fluor 594 for 60 min at room temperature, and then covered with ProLong Gold Antifade Reagent with DAPI.

Double staining of MYB and acetylated-α-tubulin

To determine whether the MYB^+ cells express acetylated-α-tubulin, we performed a double staining experiment of MYB and acetylated-α-tubulin. The ampullary sections were incubated with both MYB and acetylated-α-tubulin antibodies overnight at 4°C, washed three times with PBS, incubated with both goat anti-rabbit IgG antibody

conjugated with Alexa Fluor 488 and goat anti-mouse IgG antibody conjugated with Alexa Fluor 594 for 60 min at room temperature, and then covered with ProLong Gold Antifade Reagent with DAPI.

Statistical analysis

All the experimental data are shown as the mean ± Standard error of the mean (SEM). All the data were tested with regard to the normal distribution and the homogeneity of variance so as to check whether they were parametric or non-parametric data. A one-way analysis of variance (ANOVA) followed by Tukey's multi-comparison test were used for the parametric data. The Kruskal-Wallis test followed by the Bonferroni test were used for the non-parametric data. All the statistical analyses were performed using GraphPad Prism version 6.03 (GraphPad Software, La Jolla, CA, USA). *P* values less than 0.05 were considered to be statistically significant.

RESULTS

Changes in the numbers of ciliated, non-ciliated, and Ki67-positive cells during the estrous cycle

To clarify the cyclic changes in the numbers of non-ciliated and ciliated cells, we counted the number of cells that were positive or negative for acetylated-α-tubulin. The changes in the number of $Ki67^+$ cells during the estrous cycle were immunochemically examined. Acetylated-α-tubulin was expressed in the oviductal epithelium, but Ki67 expression was not observed in the cells that expressed acetylated-α-tubulin (Fig. 6a-c). The total number of epithelial cells did not change significantly during the estrous cycle (Fig. 6d). The number of acetylated-α-$tubulin^+$ cells (ciliated cells) was the lowest at Stage II and the highest at the Stage I (Fig. 6e, $P < 0.05$), whereas the number of acetylated-α-$tubulin^-$ cells (non-ciliated cells) did not change significantly during the estrous cycle (Fig. 6f). The number of $Ki67^+$ cells was the highest at Stage IV (Fig. 6g, $P < 0.05$).

Changes in the numbers of acetylated-α-tubulin with FOXJ1 or PAX8-positive cells during the estrous cycle

Double immunostaining for acetylated-α-tubulin and FOXJ1 showed that all the acetylated-α-$tubulin^+$ cells were positive for FOXJ1, although there were only a few acetylated-α-$tubulin^-$/$FOXJ1^+$ cells in the bovine oviductal epithelium (Fig. 7a-c). The number of acetylated-α-$tubulin^-$/$FOXJ1^+$ cells did not change significantly during the estrous cycle (Fig. 7d).

Further, we did not detect any $FOXJ1^+$ and $PAX8^+$ cells in the ampulla (Fig. 7e-g). The number of $FOXJ1^+$ cells in the ampulla was the highest in Stage I, while it was the lowest

in Stage II (Fig. 7h, $P < 0.05$). However, the number of $PAX8^+$ cells in the ampulla did not change significantly during the estrous cycle (Fig. 7i).

Changes in the numbers of MYB with FOXJ1 or PAX8-positive cells during the estrous cycle and the co-localization of MYB and Ki67

We found that MYB was expressed in the oviductal epithelial cells. Most of the MYB^+ cells expressed FOXJ1, while a few MYB^+ cells expressed PAX8 (Fig. 8a-f). Interestingly, MYB and Ki67 were not co-localized (Fig. 8g-i), which suggests that the MYB was expressed in non-proliferating cells. The number of MYB^+ cells was the highest in stage IV (Fig. 8j, $P < 0.05$).

Co-localization of MYB and acetylated-α-tubulin

Some of the MYB^+ cells were positive for acetylated-α-tubulin, while other MYB^+ cells were negative for acetylated-α-tubulin (Fig. 9). Thus, the MYB^+ cells were classified into three types of cells: $PAX8^+/MYB^+$, $FOXJ1^+/MYB^+$/ acetylated-α-$tubulin^-$, and $FOXJ1^+/MYB^+$/ acetylated-α-$tubulin^+$ cells (Fig. 9g, 9d, 10).

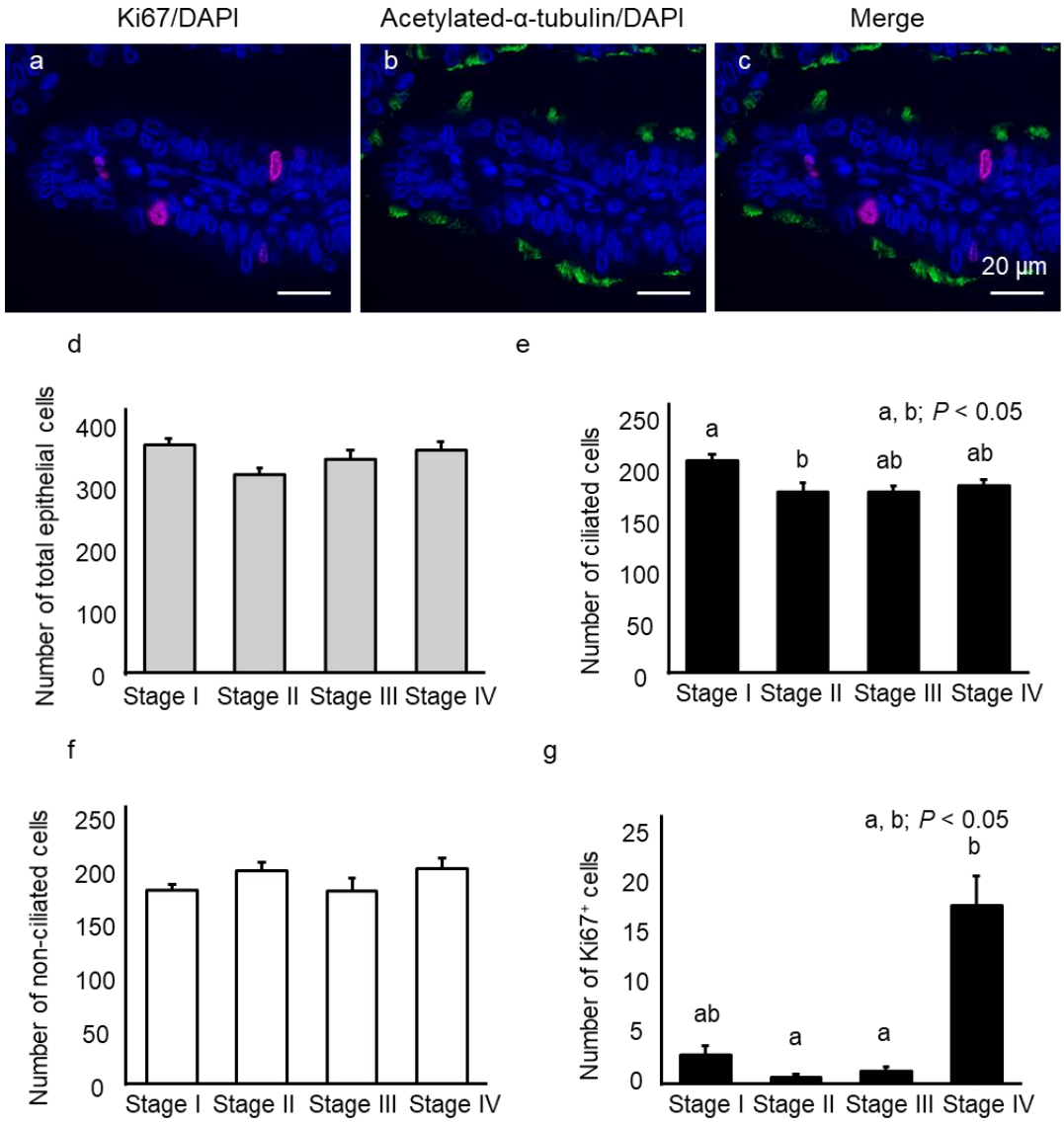

Fig. 6

Changes in the number of ciliated, non-ciliated, and Ki67^{+} cells during the estrous cycle. (**a-c**) Distributions of cells showing positive staining for acetylated-α-tubulin (red) and Ki67 (green) in the ampulla at Stage IV. Cell nuclei were counter-stained with DAPI (blue). Scale bars represent 20 μm. Changes in the number (mean ± SEM, n = 8) of (**d**) total epithelial cells, (**e**) ciliated cells, (**f**) non-ciliated cells and (**g**) Ki67^{+} cells during the estrous cycle. Different superscript letters indicate significant differences ($P < 0.05$).

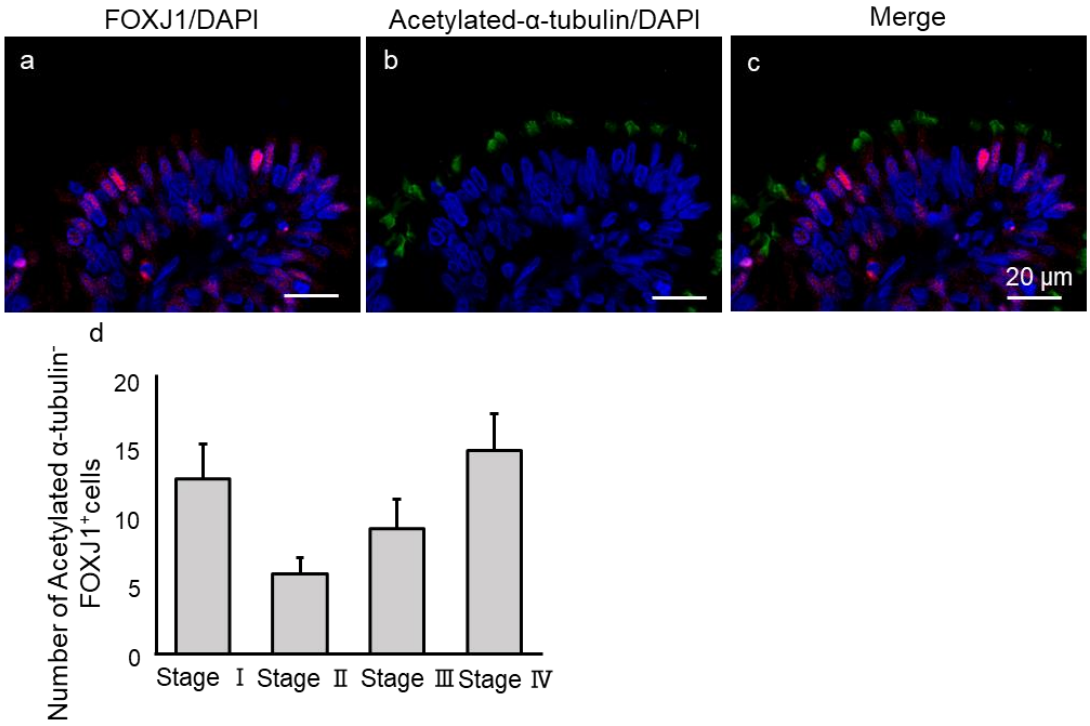
FOXJ1/DAPI
Acetylated-α-tubulin/DAPI
Merge
a
b
c
20 μm
d
Number of Acetylated α-tubulin⁻ FOXJ1⁺cells
20
15
10
5
0
Stage Ⅰ
Stage Ⅱ
Stage Ⅲ
Stage Ⅳ

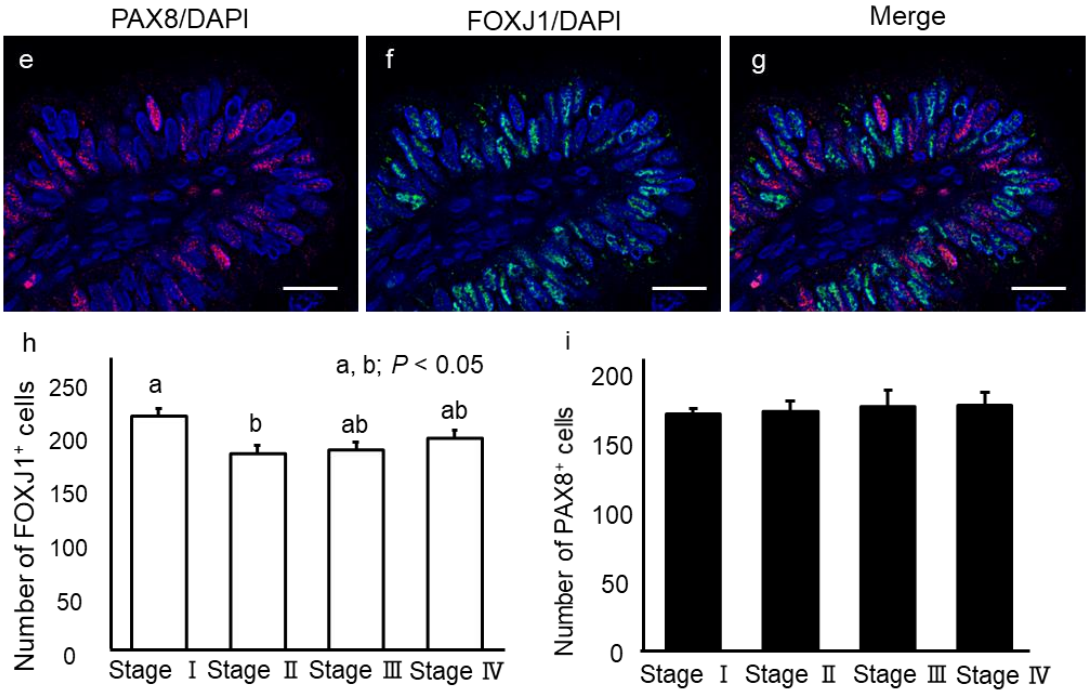
PAX8/DAPI
FOXJ1/DAPI
Merge
e
f
g
h
a, b; P < 0.05
a
b
ab
ab
Number of FOXJ1⁺ cells
250
200
150
100
50
0
Stage Ⅰ
Stage Ⅱ
Stage Ⅲ
Stage Ⅳ
i
Number of PAX8⁺ cells
200
150
100
50
0
Stage Ⅰ
Stage Ⅱ
Stage Ⅲ
Stage Ⅳ

Fig. 7

Changes in the number of acetylated-α-tubulin with FOXJ1^{+} cells and PAX8^{+} cells during the estrous cycle. (**a-c**) Distributions of cells showing positive staining for acetylated-α-tubulin (green) and FOXJ1 (red) in the ampulla at Stage IV. Cell nuclei were counter-stained with DAPI (blue). (**d**) Changes in the number (mean ± SEM, n = 8) of FOXJ1^{+} cells during the estrous cycle. (**e-g**) Distributions of cells showing positive staining for PAX8 (red) and FOXJ1 (green) in the ampulla at Stage IV. Cell nuclei were counter-stained with DAPI (blue). Scale bars represent 20 μm. Changes in the number (mean ± SEM) of (**h**) FOXJ1^{+}/acetylated-α-tubulin^{-} (n = 12) and (**i**) PAX8 positive cells (n = 8) during the estrous cycle. Different superscript letters indicate significant differences ($P < 0.05$)

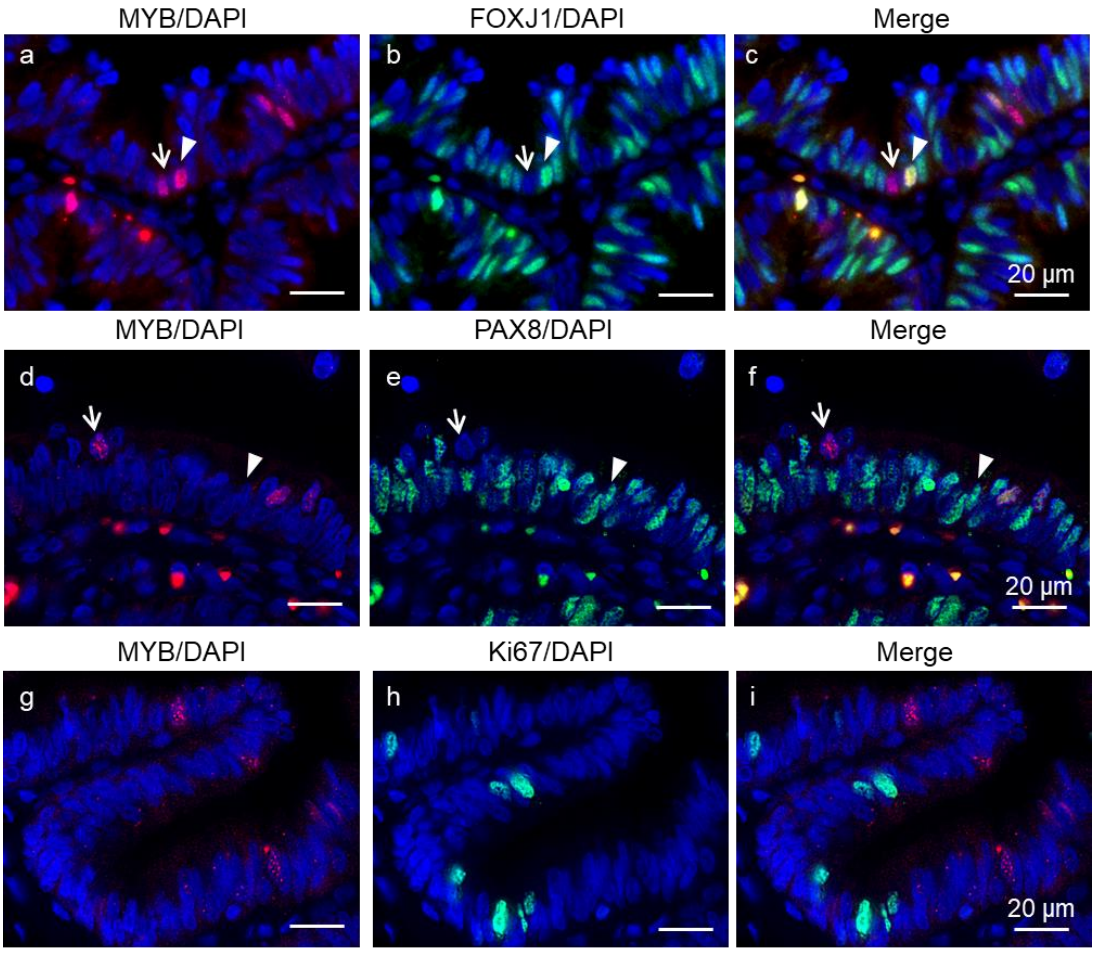
MYB/DAPI
FOXJ1/DAPI
Merge
a
b
c
20 μm
MYB/DAPI
PAX8/DAPI
Merge
d
e
f
20 μm
MYB/DAPI
Ki67/DAPI
Merge
g
h
i
20 μm

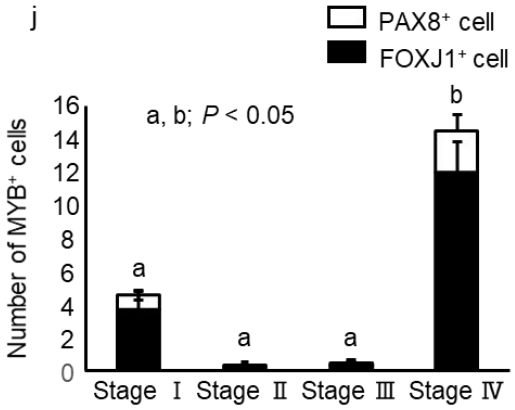
j
PAX8⁺ cell
FOXJ1⁺ cell
a, b; P < 0.05
Number of MYB⁺ cells
16
14
12
10
8
6
4
2
0
a
a
a
b
Stage Ⅰ
Stage Ⅱ
Stage Ⅲ
Stage Ⅳ

Fig. 8

Changes in the number of MYB with FOXJ1 or PAX8-positive cells during the estrous cycle and co-localization of MYB and Ki67. (**a-c**) Distributions of cells showing positive staining for MYB (red) and FOXJ1 (green). Arrows indicate the cells that were double-positive for MYB and FOXJ1, and arrowheads indicate the cells that were positive for MYB and negative for FOXJ1. (**d-f**) Distributions of cells showing positive staining for MYB (red) and PAX8 (green). Arrowheads indicate the cells that were double-positive for MYB and PAX8. Some MYB^+ cells were negative for PAX8 (arrow). (**g-i**) Distributions of cells showing positive staining for MYB (red) and Ki67 (green). Ki67 was not detected in MYB-expressing cells. Cell nuclei were counter-stained with DAPI (blue). Scale bars represent 20 μm. (**j**) The number of MYB^+ cells (mean ± SEM, n = 8) during the estrous cycle. The black bars indicate the number of cells that were positive for MYB and FOXJ1, and the white bars indicate the number of cells that were positive for MYB and PAX8. Different superscript letters indicate the significant differences ($P < 0.05$).

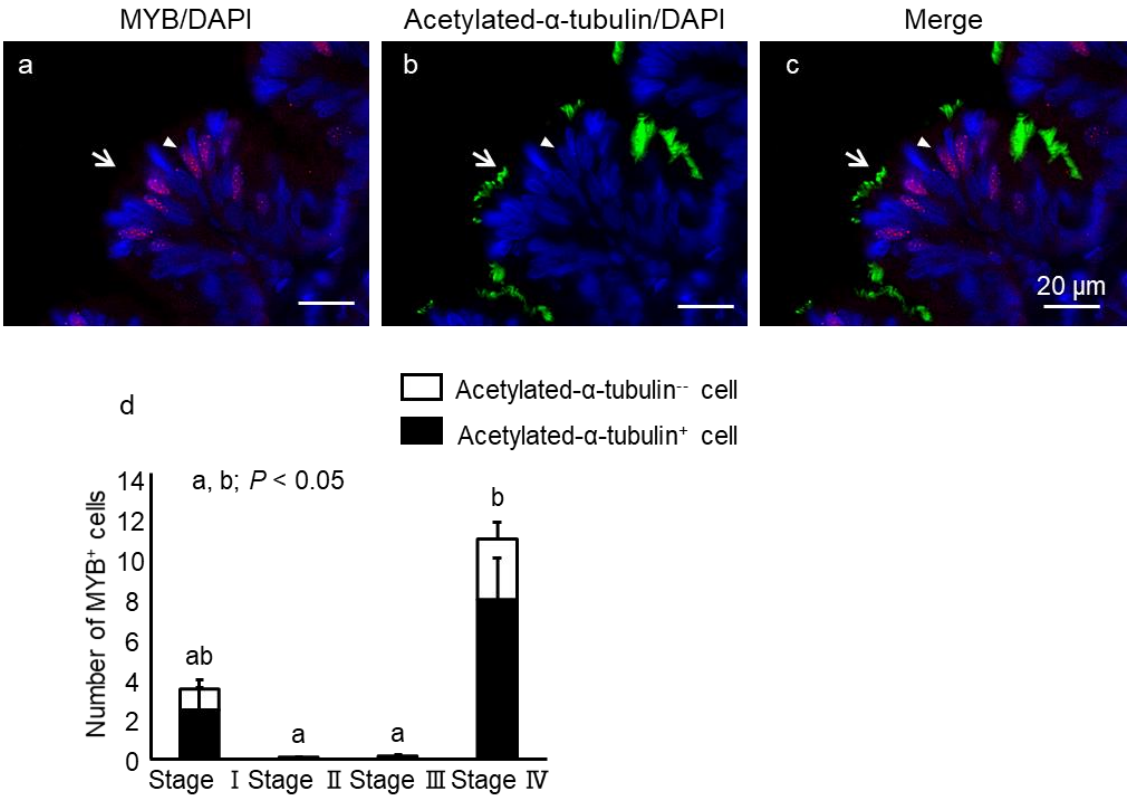

Fig. 9

Co-localization of MYB and acetylated-α-tubulin during the estrous cycle. (**a-c**) Distributions of cells showing positive staining for MYB (red) and acetylated-α-tubulin (green) in the ampulla at Stage IV. Arrows indicate acetylated-α-tubulin and MYB double-positive cells, while some MYB^+ cells were negative for acetylated-α-tubulin (arrowhead). Cell nuclei were counter-stained with DAPI (blue). (**d**) Changes in the number (mean ± SEM, n = 8) of MYB^+ cells during the estrous cycle. The black bars indicate the number of cells that were double-positive for MYB and acetylated-α-tubulin, and the white bars indicate the number of cells that were positive for MYB and negative for acetylated-α-tubulin. Different superscript letters indicate significant differences ($P < 0.05$).

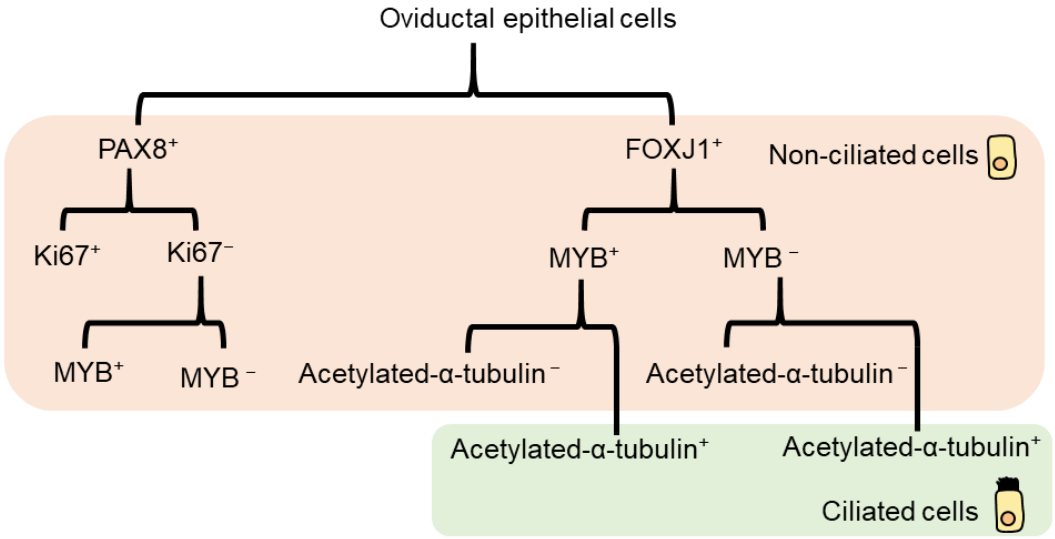

Fig. 10

Classification of bovine oviductal epithelial cells. The bovine oviductal epithelium is composed of ciliated (acetylated-α-tubulin^{+}) and non-ciliated (acetylated-α-tubulin^{-}) cells morphologically, but based on immunological classification, there are seven type of the cells in oviductal epithelium.

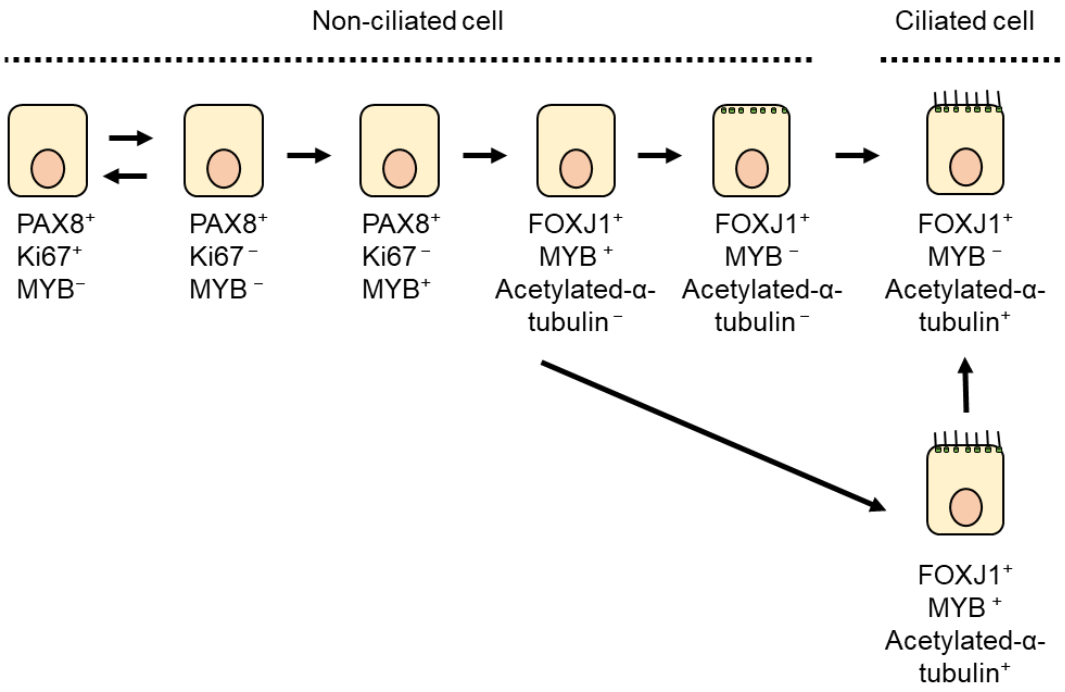

Fig. 11

Proposed model for ciliogenesis in the bovine oviductal epithelium. This illustration shows the ciliogenesis process in the bovine oviductal epithelium, which was speculated from the results of the present study together with the previous studies on the airway duct epithelia. At least seven types of cells at different stages of ciliogenesis are existed in the oviductal epithelium. $PAX8^{+}/Ki67^{-}/MYB^{+}$ cells are derived from $PAX8^{+}/Ki67^{+}/MYB^{-}$ cells, and then these cells express MYB and FOXJ1. $FOXJ1^{+}/MYB^{+}$/acetylated-α-$tubulin^{-}$ cells are transformed into $FOXJ1^{+}/MYB^{-}$/acetylated-α-$tubulin^{-}$ cells or $FOXJ1^{+}/MYB^{+}$/acetylated-α-$tubulin^{+}$ cells. $FOXJ1^{+}/MYB^{-}$/acetylated-α-$tubulin^{-}$ cells might be the mature ciliated cells in the bovine oviduct.

DISCUSSION

Several morphological and functional changes occur during the estrous cycle in the oviductal epithelium, and these changes are responsible for providing a suitable micro-environment for gamete transport, fertilization, and early embryo development. However, the mechanism of the cyclic morphological changes that occur in the bovine oviduct has not yet been elucidated. Our previous study showed that the proportion of $FOXJ1^+$ cells changes during the estrous cycle, and that only the $FOXJ1^-$ cells undergo proliferation [65], suggesting that oviductal non-ciliated cells can give rise to ciliated cells. The present study shows that ciliogenesis is a multistep process that is closely related to the estrous cycle in the bovine oviduct.

Ciliogenesis involves the following stages: (1) cell cycle exit, (2) amplification of hundreds of centrioles, and (3) migration of those centrioles and the docking at the apical surface of the ciliated cells [75][. Ciliogenesis is coordinated by a number of transcription factors, including MYB and FOXJ1 [76]. MYB is a member of the MYB family of proteins, which is encoded by the *c-MYB* that is involved in centriole amplification during ciliogenesis [62]. FOXJ1 regulates both axoneme growth and basal body docking with the apical surface [77]. Mature ciliated cells exhibit a multi-ciliated structure, which is labeled with acetylated-α-tubulin on the apical plasma membrane [78]. To clarify the types of epithelial cells that exist in the oviduct as well as the dynamic changes that occur in their populations, the numbers of cells positive for acetylated-α-tubulin (cilia marker), FOXJ1 and MYB (markers of ciliogenesis), Ki67 (proliferation marker), and PAX8 (non-ciliated cell marker) in the epithelial cells during the estrous cycle were immunohistochemically examined in the present study.

We found that all the ampullary oviductal epithelial cells expressed either FOXJ1

or PAX8 (Fig.7e-g) and all the acetylated-α-tubulin$^+$ cells were positive for FOXJ1, and there were a few acetylated-α-tubulin$^-$/FOXJ1$^+$ cells in the bovine oviduct (Fig. 7a-c). Moreover, MYB was found to be expressed in both the FOXJ1$^+$ and PAX8$^+$ cells. Some of the MYB$^+$/FOXJ1$^+$ cells were positive for acetylated-α-tubulin (Fig. 9a-c). These results showed that the MYB$^+$ cells could be classified into three types of cells, namely PAX8$^+$/MYB$^+$, FOXJ1$^+$/MYB$^+$/acetylated-α-tubulin$^-$ and FOXJ1$^+$/MYB$^+$/acetylated-α-tubulin$^+$ (Fig. 10). Based on the results of the double staining of MYB and Ki67 (Fig. 8g-i), the PAX8$^+$/Ki67$^+$ cells and PAX8$^+$/MYB$^+$ cells represented independent populations in the bovine oviduct (Fig. 8g-i), as previously reported in the airway duct [79,62]. In the light of all these results, we identified at least seven types of cells at different translational/transcriptional states in the bovine oviductal epithelium (Fig. 10). Since intermediate cells, which are morphologically immunologically distinct have previously been identified in the airway [68], these types of oviductal epithelial cells found in this study may also be considered to be intermediate cells in the process of ciliogenesis.

Based on the results of previous studies and those of the present study, we tried to speculate the ciliogenesis process in the oviduct. Recently, it has been reported that oviductal non-ciliated cells (PAX8$^+$ cells) give rise to ciliated cells, and PAX8$^+$/acetylated-α-tubulin$^+$ cells exist in the mouse oviduct [57]. In the present study, we could not find any PAX8$^+$/acetylated-α-tubulin$^+$ cells in the bovine oviduct, and all the acetylated-α-tubulin$^+$ cells were FOXJ1$^+$ and PAX8$^-$. These findings suggest that cell types observed in ciliogenesis depend on the species. Intriguingly, bovine oviductal epithelial cells expressed either FOXJ1 or PAX8, and MYB was expressed in both PAX8$^+$ cells and FOXJ1$^+$ cells. In the airway, MYB is able to induce FOXJ1 expression, and acetylated-α-tubulin$^+$ cells are derived from FOXJ1$^+$ cells [80]. As the deletion of MYB

results in the failure of cilia formation in the airway and kidney, MYB is one of the most important factors associated with ciliogenesis in such tissues [62,81,82]. The highest numbers of $Ki67^+$ and MYB^+ cells were observed in Stage IV (Fig.6g, 8j), whereas the numbers of $FOXJ1^+$ and acetylated-α-$tubulin^+$ cells gradually increased toward following Stage I (Fig.6e, 8j). Since this diphasic increase in the numbers of MYB^+ cells, $FOXJ1^+$ cells, and acetylated-α-$tubulin^+$ cells is the same as the temporal pattern of ciliogenesis observed in the airway [83,84], $FOXJ1^+$ cells are believed to be derived from some MYB^+ cells and they ultimately become acetylated-α-$tubulin^+$ cells in the oviduct. Although MYB^+ cells and acetylated-α-$tubulin^+$ cells represent independent populations in the airway epithelium [81], some MYB^+ cells were positive for acetylated-α-tubulin in the bovine oviduct (Fig. 9a-c). Moreover, these MYB^+/acetylated-α-$tubulin^+$ cells could only be detected in Stage I and Stage IV (Fig. 9d), and the number of these cells was the lowest among the seven cell populations identified in this study. Although MYB is expressed during centriole amplification, its expression is lost as centrioles dock at the apical membrane [62]. Given that MYB is transiently expressed during ciliogenesis in the airway, it is reasonable to assume that acetylated-α-$tubulin^+$/MYB^+/$FOXJ1^+$ cells eventually exhibit decreased MYB expression and become acetylated-α-$tubulin^+$/MYB^-/$FOXJ1^+$ cells in the oviduct.

The double immunostaining experiments involving MYB and PAX8 or Ki67 revealed that there were three types of $PAX8^+$ cells in the bovine oviductal epithelium, namely $PAX8^+$/$Ki67^-$/MYB^-, $PAX8^+$/$Ki67^+$/MYB^-, and $PAX8^+$/$Ki67^-$ /MYB^+. However, there were no MYB and Ki67 double-positive cells present (Fig. 8g-i). Given that ciliogenesis occurs in the non-proliferating cells in the airway [85,86], it is reasonable to infer that some $PAX8^+$/$Ki67^+$/MYB^- cells proliferate, and further, that

$PAX8^+/Ki67^-/MYB^+$ cells are derived from those proliferating cells. Collectively, the seven types of oviductal epithelial cells identified in this study appear to initiate ciliogenesis from Stage IV to the following Stage I through the complex ciliogenesis steps shown in Fig. 11. On the other hand, it has been reported that ciliated cells trans- and re-differentiate during tissue repair in the airway duct of mice and humans [87,88], although this has never been discovered in their oviduct. However, in the current study of the bovine oviduct it has not demonstrated whether this mechanism was involved in the decrease in the number of ciliated cells from Stage I to Stage II. In the present study, it remains unclear whether oviductal epithelial cells undergo deciliation or not. Nonetheless, the same mechanism might also exist in the oviduct. Further research will be needed to clarify this matter.

In the airway, following damage caused by viral or bacterial infection, the epithelium is rapidly repaired in just three days [68]. However, the results of this study suggest that since ciliogenesis in the oviduct was initiated at Stage IV and terminated at the following Stage I at least one week is necessary for ciliogenesis in the oviduct. These findings imply that unlike the rapid ciliogenesis seen in the airway in response to infection, ciliogenesis in oviductal epithelial cells gradually proceeds toward ovulation. In the airway, inflammatory cytokines such as IL-6 are known to contribute to the rapid ciliogenesis seen in the epithelial cells [89], whereas the regulation of ciliogenesis by inflammatory factors in the oviduct has not yet been reported. Moreover, ciliogenesis in the airway epithelial cells is regulated by Wnt signaling [90]. Recently, similar to the situation in the airway, it has been reported that oviductal non-ciliated cells ($PAX8^+$ cells) give rise to ciliated cells, and further that this process is controlled by Wnt signaling in mice [57]. Interestingly, the expression of Wnt-related molecules is regulated by the

ovarian steroid hormone in the oviduct [78,91]. Since ciliogenesis is associated with the estrous cycle, ovarian steroid hormones may be involved in ciliogenesis in the bovine oviduct. However, the precise mechanism in this regard has not yet been elucidated, and the factors that regulate ciliogenesis will need to be further clarified in the bovine oviduct.

In conclusion, bovine oviductal epithelial cells can be morphologically classified into ciliated and non-ciliated cells. However, based on immunological classifications, at least seven types of cells at different translational/transcriptional states are present in the oviductal epithelium, and their numbers are regulated by the estrous cycle. This cyclic event might provide the optimal environment for gamete transport, fertilization and embryo development.

SUMMARY

The oviductal epithelium is composed of ciliated and non-ciliated cells. The proportions of these cells change during the estrous cycle. However, the mechanism underlying this cyclic change in the cell proportions remains unclear. Our previous study indicated that ciliated cells are derived from non-ciliated cells. Here, we aimed to investigate the mechanism regulating the changes in the populations of ciliated and non-ciliated cells during the estrous cycle. To this end, we examined the numbers of cells that were positive for acetylated-α-tubulin (cilia marker), Ki67 (proliferation marker), PAX8 (non-ciliated cell marker), and FOXJ1 and MYB (ciliogenesis markers) in the epithelial cells at four different estrous stages (Stage I: Days 1-4 after ovulation, Stage II: Days 5-10, Stage III: Days 11-17, and Stage IV: Days 18-20) by immunohistochemistry. The oviductal epithelial cells expressed either FOXJ1 or PAX8. All the acetylated-α-tubulin^{+} cells were positive for FOXJ1, although there were a few acetylated-α-tubulin^{-}/FOXJ1^{+} cells. MYB was expressed in both the FOXJ1^{+} and PAX8^{+} cells, but it was not expressed in the Ki67^{+} cells. The numbers of Ki67^{+} and MYB^{+} cells were the highest in Stage IV, while the numbers of FOXJ1^{+} and acetylated-α-tubulin^{+} cells were the highest in the following Stage I, suggesting that ciliogenesis is associated with the estrous cycle. Thus, based on immunological classification, the oviductal epithelium contains at least seven types of cells at different translational/transcriptional states, and their number is regulated by the estrous cycle. This cyclic event might provide an optimal environment for gamete transport, fertilization, and embryonic development.

CHAPTER 4
Ciliogenesis of bovine oviductal epithelial cells cultured on air-liquid interface culture

INTRODUCTION

Two types of the cells, ciliated and non-ciliated cells, are present in the oviductal epithelium, and the number of them changes during the estrous cycle [34]. However, the mechanisms this cyclic event within the oviduct are still not clearly elucidated. The results of chapter 3 suggested that the oviductal epithelium contains at least seven types of cells at different translational/transcriptional states in terms of immunological classification, and ciliogenesis in the bovine oviductal epithelial cells is associated with the estrous cycle. However, the detailed ciliogenesis mechanisms in the bovine oviductal epithelial cells has not been manifested. Thus, in this chapter, we investigated the expression pattern of ciliogenesis associated factors in the bovine oviductal epithelial cells *in vivo* compared with the *in vitro* state and during cell culture.

In vitro culture systems of bovine oviductal epithelial cells have been developed in several species [92-96]. However, when oviductal epithelial cells are cultured on the plastic plate, cells lose cell polarity, ciliation, secretory activity, and functional characteristics [97,98]. Thus, this culture system did not precisely mimic the oviduct *in vivo*. Several cell culture models for primary bovine oviductal epithelial cells that develop polarized epithelial cells were established to reveal physiological event [98-100]. Recently, air-liquid interface (ALI) culture models are frequently used for variety of epithelia, such as epidermal, airway, and nasal epithelium [101-103]. ALI culture is a method of cell culture in which cells are grown on porous filter and the apical surface of the cultured cells is exposed to air by removing the culture medium. In this condition,

epithelial cells can obtain apical-basal polarity [32,104-106]. The ALI culture is the most commonly used approach to study the ciliogenesis of airway epithelial cells [107]. Similar to epithelial cells in the airway, bovine oviductal epithelial cells cultured by ALI can establish polarity, and undergo ciliogenesis in approximately 2-3 weeks [108-110]. During the ALI culture, epithelial cells might be formed cilia through a stepwise process of ciliogenesis. However, the detailed process of ciliogenesis in the ALI cultured bovine oviductal epithelial cells has not been elucidated.

The aim of this study is to clarify the ciliogenesis in the bovine oviductal epithelial cells. To achieve the purpose, we investigated the temporal ciliogenesis of bovine oviductal epithelial cells grown at ALI culture, and compared with *in vitro* situation.

MATERIAL AND METHODS

Isolation of bovine oviductal epithelial cells

The bovine oviducts were collected from a local abattoir within 10–20 min after the exsanguination. A careful examination was performed so that any infected ovaries or uteri could be omitted from the experiment. Based on ovarian and uteri morphology, oviducts were classified at four different stages of the estrous cycle (Stage I, Days 1–4; Stage II, Days 5–10; Stage III, Days 11–17; Stage IV, Days 18–20), as previously described [36,37,74]. Ampullary oviductal tissues collected at Stage III were utilized for cell culture. Oviducts were trimmed into infundibulum, ampulla, and isthmus. The epithelial cells were isolated from the ampullary section of oviduct. Epithelial cells were obtained by squeezing the oviduct with forceps [109]. Cells were suspended in 5 ml Hank's balanced salt solution (HBSS) containing 66 units/ml collagenase (Wako), 80 units/ml deoxyribonuclease I (BBI Enzymes, Cardiff, UK), 100 IU/mL penicillin (Meiji Seika Pharma, Tokyo, Japan) and 100 µg/mL streptomycin (Meiji Seika Pharma), and incubated at 37℃ for 30 min. After incubation, cells were filtered through metal meshes (77 µm) to remove undissociated tissue fragments. The filtered were washed by centrifugation (180 x g for 8 min at 30℃) with Tris-buffered ammonium chloride (pH 7.5) to remove hemocytes, and DMEM/Ham's F-12 (Invitrogen, Carlsbad, CA,USA). After the washes, the cells were counted with hemocytometer. Cell viability was higher than 95 % as assessed by 0.5 % (wt/vol) trypan blue dye exclusion.

Media used in this culture procedure are modifications of a protocol previously reported [111,106]. The basic medium is DMEM/Ham's F-12 supplemented with 5 % Fetal Bovine Serum (Biowest, Riverside, MO, USA), 10 µg/mL insulin (Sigma Aldrich),

5 μg/mL holo-transferrin (BBI solutions), 25 ng/mL Epidermal Growth Factor (Sigma Aldrich), 30 μg/mL Bovine Pituitary Extract (Life technology), 0.05 μM ec23 (reprocell, Japan), 20 mg/mL gentamicin (Invitrogen), and 2 mg/mL amphotericin B (Sigma Aldrich).

Isolated epithelial cells were resuspended in basic medium at a concentration of 1.0 x 10^6 cells/250 μl and seeded on transwell inserts (PET membrane, 0.4 μm pore size, 24 well plate, Corning, NY, USA) coated with bovine type IV collagen (0.5 μg/well; Nippi, Japan). Cells were initially cultured under the immersed condition by adding 250 μL of basic medium apically and 1 mL of basic medium in the basal chamber until they reached confluence. When the epithelial cells reached confluence, the medium from inside the insert was removed, allowing the cells to be in contact with the medium only from basolateral side. Cells were incubated in a humidified atmosphere at 38.5 ℃ and 5% CO_2. The medium was changed every 2 days and culture for 2 weeks.

Epithelial cells for analysis of mRNA expression were added to 200 μl RNAiso Plus reagent (Takara Bio, Japan) for RNA extraction, and stored at -80℃.

Total RNA extraction and reverse transcription

Total RNA was extracted from the oviductal epithelial cells using RNAiso Plus reagent, according to the manufacturer's directions. One microgram of total RNA per sample was used to synthesize cDNA by using ReverTra Ace RT Master Mix with gDNA Remover (TOYOBO, Japan).

Quantitative reverse transcription polymerase chain reaction

Quantifications of mRNA expressions were determined by quantitative RT-PCR using AriaMx (Agilent Technologies) and Brilliant III Ultra-Fast SYBR Green QPCR

Master Mixes (Agilent Technologies). The reaction mixture contained Brilliant III Ultra-Fast SYBR Green QPCR Master Mixes, 1 μM of each forward and reverse primer, and 1 ng of reverse transcribed total RNA in a final reaction volume of 20 μl. PCR was performed under the following conditions: 95°C for 30 s, 45 cycles of 95°C 15 s, corresponding annealing temperature for 15 s, 72°C 10 s. All the primer sequences and their annealing temperature are listed in Table 1. The specificity of each primer set was confirmed by running the PCR products on a 2.0% agarose gel. To standardize the relative level of expression of each mRNA, three potential housekeeping genes, β-actin (*ACTB*), 18S ribosomal RNA (*18S rRNA*), and glyceraldehyde-3-phosphate dehydrogenase (*GAPDH*) were initially tested. *GAPDH* was found to be most suitable of three genes by Normfinder software (http://moma.dk/normfindersoftware), and selected as the internal control in our experiments. Amplification efficiencies of all the primers were checked by the determination of Ct values for dilution series of the target template. Efficiencies of all the primers were 80-100%. We used serial dilutions of extracted PCR products for preparation of standard curve.

Immunohistochemistry and Cell counting

Cultured epithelial cells were fixed in 4% paraformaldehyde for 2 hours at 4 ℃, permeabilized with 0.1% Triton X-100 in PBS for 30 minutes, and incubated in 5% BSA-PBS for 1 hour at room temperature to block non-specific binding. After blocking, 1st antibodies were added apically to Transwell and incubated overnight at 4 ℃. The following primary antibodies were used: rabbit anti-acetylated-α-tubulin (1:500, ab179484, Abcam), rabbit anti-FOXJ1 (1:00, AMAb91255, Sigma Aldrich), mouse anti-

FOXJ1 (1:100, HPA005714, Sigma Aldrich), mouse anti-Ki67 (1:200, M7240, Dako-Cytomation, Glostrup), and mouse anti-MYB (1:100, sc-74512, Santa Cruz, Santa Cruz). After washing with PBS, incubated with both goat anti-rabbit IgG antibody conjugated with Alexa Fluor 488 and goat anti-mouse IgG antibody conjugated with Alexa Fluor 594 for 60 min at room temperature. The membranes were cut from the inserts and placed on glass slides, and then covered with ProLong Gold Antifade Reagent with DAPI (P36935, Life Technologies). The sections were mounted on an Olympus FSX100 (Olympus) and observed under the 200x objective or higher. Each digital picture was captured as a TIF file. Cell counting was performed manually on immunohistochemistry images using ImageJ software and 3 areas from x200 magnification fields.

Statistical Analysis

All the statistical analysis was performed using GraphPad Prism version 6.03 (GraphPad Software). All data are presented as the mean ± SEM. All the data were tested with regard to the normal distribution and the homogeneity of variance so as to check whether they were parametric or non-parametric data. A one-way ANOVA was performed with Dunnett's multiple comparisons test after logarithm transformation of data to evaluate each gene expression level differences between groups. The Kruskal-Wallis test followed by the Bonferroni test were used for the non-parametric data.

Target gene	Primer sequence (5'-3')	Accession number	Product size (bp)	Temperature (˚C)
ACTB	Forward: CAGCAAGCAGGAGTACGATG	AY141970	137 bp	60
	Reverse: AGCCATGCCAATCTCATCTC			
18S rRNA	Forward: TCGCGGAAGGATTTAAAGTG	AY779625	141 bp	60
	Reverse: AAACGCCTACCACATCCAAG			
GAPDH	Forward: CACCCTCAAGATTGTCAGCA	NM_001034034.2	103 bp	60
	Reverse: GGTCATAAGTCCCTCCACGA			
MYB	Forward: ATCGAACAGATGTCCAGTGC	NM_175050.1	191 bp	58
	Reverse: ATGCCACCTCTCCCTACATT			
FOXJ1	Forward: AGCAAGGCCACCAAGATCACC	NM_001192076.1	144 bp	56
	Reverse: CCGAGGCACCTTGATGAAGCAC			

Table. 1 Primers used for in quantitative RT-PCR

RESULTS

Time course of cell proliferation and ciliogenesis during ALI culture

Proliferation and ciliogenesis of bovine epithelial cells were assessed using immunostaining of Ki67 and acetylated-α-tubulin, respectively. Ki67 expression did not overlap with that of PAX8 (Fig. 12a-i). We observed acetylated-α-tubulin^{+} cells in the ALI cultured bovine oviductal epithelial cells (j-l).

The highest number of Ki67^{+} cells observed at day 0 (Fig. 12n). The average cell number per field was shown to plateau between day 2 and day 10 (Fig. 12m), suggesting that cells were confluency. Once the number of acetylated-α-tubulin^{+} cells had reached a peak at day 2 post-ALI, after that the number of acetylated-α-tubulin^{+} cells dramatically decreased during the ALI culture (Fig. 12o).

MYB and FOXJ1 mRNA expression in the bovine oviductal epithelial cells

The mRNA expression of FOXJ1 was highest at days 4 post-ALI ($P < 0.05$). On the other hand, MYB mRNA expression did not change significantly during the ALI culture (Fig. 13).

Epithelial cells composition during ALI culture

We compared the expression pattern of MYB^{+}, FOXJ1^{+}, and PAX8^{+} cells in the bovine oviductal epithelial cells during the ALI culture. There were FOXJ1^{+} cells, PAX8^{+} cells, and MYB^{+} cells in the ALI cultured oviductal epithelial cells (Fig. 14a-i). The number of PAX8^{+} cells gradually increased with culture time (Fig. 14j; $P = 0.07$). In contrast, the number of FOXJ1^{+} cells became the largest at day 4 (not significantly different) (Fig. 14k).

We observed cells that were double positive and negative for both FOXJ1 and PAX8 in the bovine oviductal epithelial cells during the ALI culture (Fig. 14a-i). The number of $FOXJ1^{-}/PAX8^{-}$ cells was increased significantly from day 2 to day 6 (Fig. 14l). Whereas, the number of FOXJ1 expressing cells began to decrease from day 6, the number of $FOXJ1^{-}/PAX8^{-}$ cells continued to increase (Fig. 14l).

MYB^{+} cells were observed in the ALI cultured bovine oviductal epithelial cells (Fig. 15a-i). The number of cells positive for MYB was highest at day 6, and decreased toward the days 14. Most of MYB^{+} cells were positive for PAX8 (Fig. 15j).

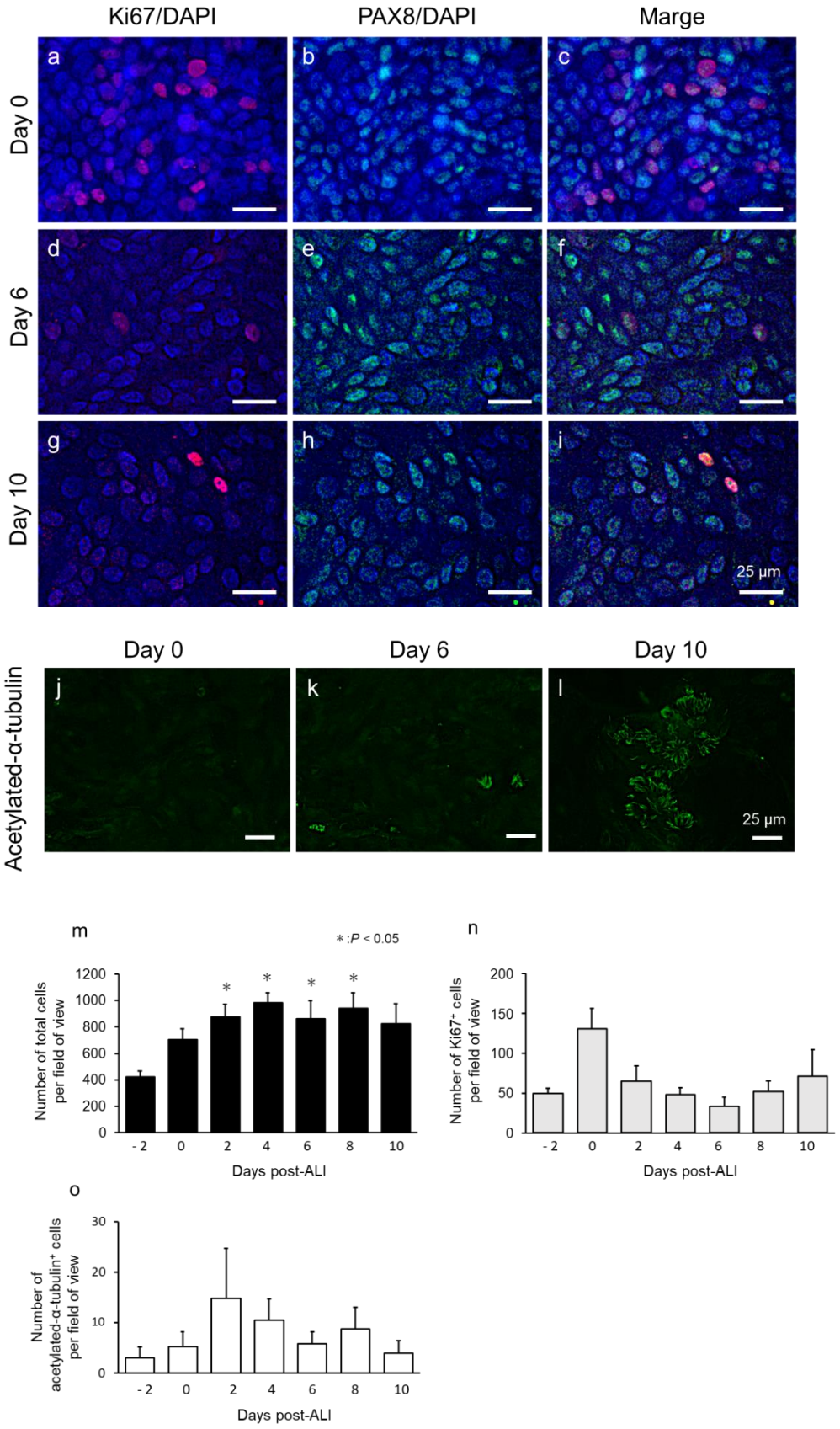
Ki67/DAPI
PAX8/DAPI
Marge
Day 0
Day 6
Day 10
a
b
c
d
e
f
g
h
i
25 μm
Day 0
Day 6
Day 10
Acetylated-α-tubulin
j
k
l
25 μm
m
*:P < 0.05
Number of total cells per field of view
Days post-ALI
n
Number of Ki67+ cells per field of view
Days post-ALI
o
Number of acetylated-α-tubulin+ cells per field of view
Days post-ALI

Fig. 12

Localization of Ki67, PAX8, and acetylated-α-tubulin in ALI cultured bovine oviductal epithelial cells. (**a-i**) Distributions of cells showing positive staining for Ki67 (red) and PAX8 (green) in ALI cultured bovine oviductal epithelial cells. Cell nuclei were counter-stained with DAPI (blue). (**j-l**) Distributions of cells showing positive staining for acetylated-α-tubulin (green) in ALI cultured bovine oviductal epithelial cells. Scale bars represent 25 μm. Change in the number of (mean ± SEM, n = 7) (**m**) total epithelial cells, (**n**) $Ki67^+$ cells, and (**o**) acetylated-α-$tubulin^+$ cells per field of view. The asterisk indicates $P < 0.05$ when compared to before onset of ALI (Days -2).

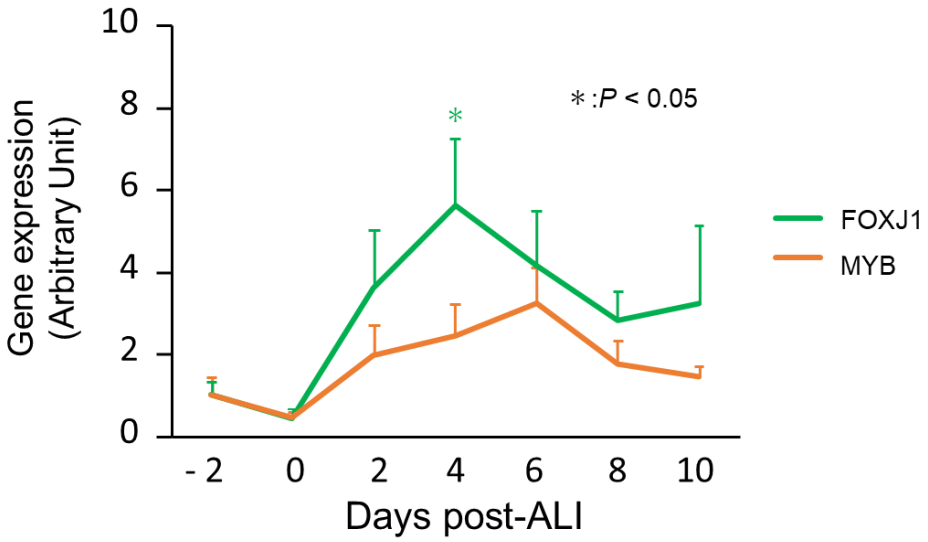

Fig. 13

Change in the expression of ciliogenesis related genes (MYB and FOXJ1) during the ALI culture. The line chart shows that MYB (orange) and FOXJ1 (green) mRNA levels in the ALI cultured bovine oviductal epithelial cells. The asterisk indicates $P < 0.05$ when compared to before the onset of ALI (Days -2).

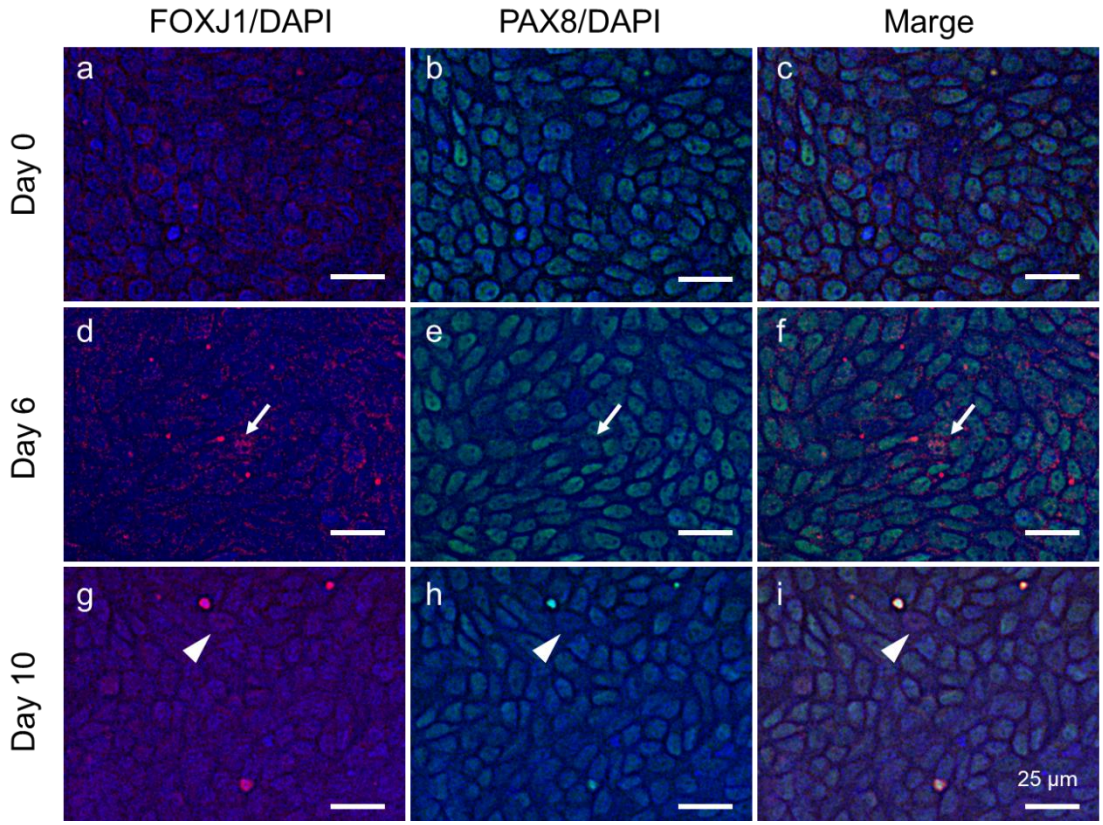
FOXJ1/DAPI
PAX8/DAPI
Marge
Day 0
Day 6
Day 10
a
b
c
d
e
f
g
h
i
25 μm

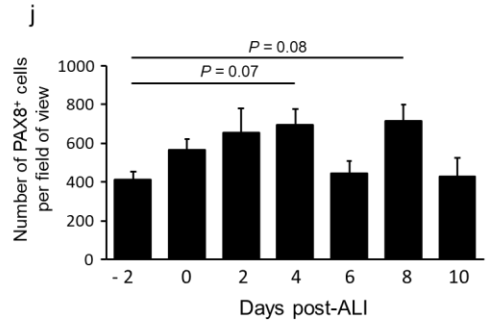
j
P = 0.08
P = 0.07
Number of PAX8+ cells per field of view
1000
800
600
400
200
0
- 2
0
2
4
6
8
10
Days post-ALI

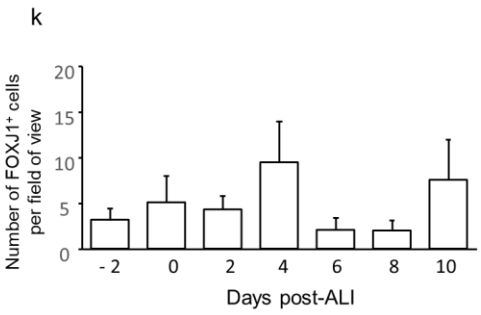
k
Number of FOXJ1+ cells per field of view
20
15
10
5
0
- 2
0
2
4
6
8
10
Days post-ALI

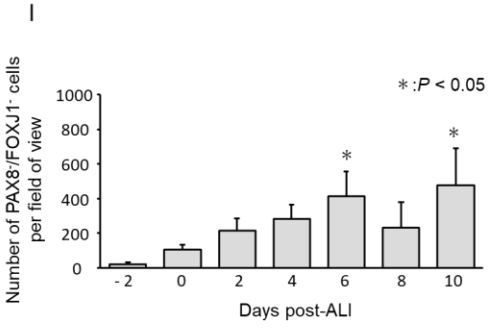
l
Number of PAX8-/FOXJ1- cells per field of view
*:P < 0.05
1000
800
600
400
200
0
*
*
- 2
0
2
4
6
8
10
Days post-ALI

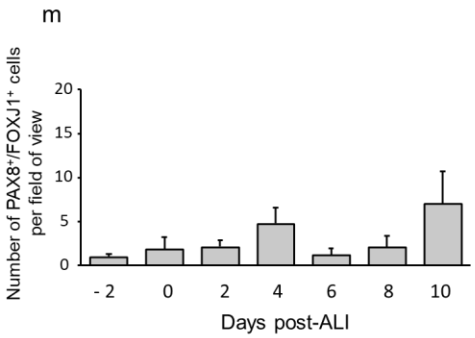
m
Number of PAX8+/FOXJ1+ cells per field of view
20
15
10
5
0
- 2
0
2
4
6
8
10
Days post-ALI

Fig. 14

Co-localization of FOXJ1 and PAX8 in ALI cultured bovine oviductal epithelial cells (**a-i**). Distributions of cells showing positive staining for FOXJ1 (red) and PAX8 (green) in the ALI cultured bovine oviductal epithelial cells. Arrows indicate the cells that were double-positive for MYB and PAX8, and arrowheads indicate the cells that were positive for MYB and negative for PAX8. Cell nuclei were counter-stained with DAPI (blue). Scale bars represent 25 μm. Changes in the number of (mean ± SEM, n = 7) (**j**) $PAX8^+$ cells, (**k**) $FOXJ1^+$ cells, (**l**) $PAX8^-/FOXJ1^-$ cells, and (**m**) $PAX8^+/FOXJ1^+$ cells per field of view. The asterisk indicates $P < 0.05$ when compared to before the onset of ALI (Days -2).

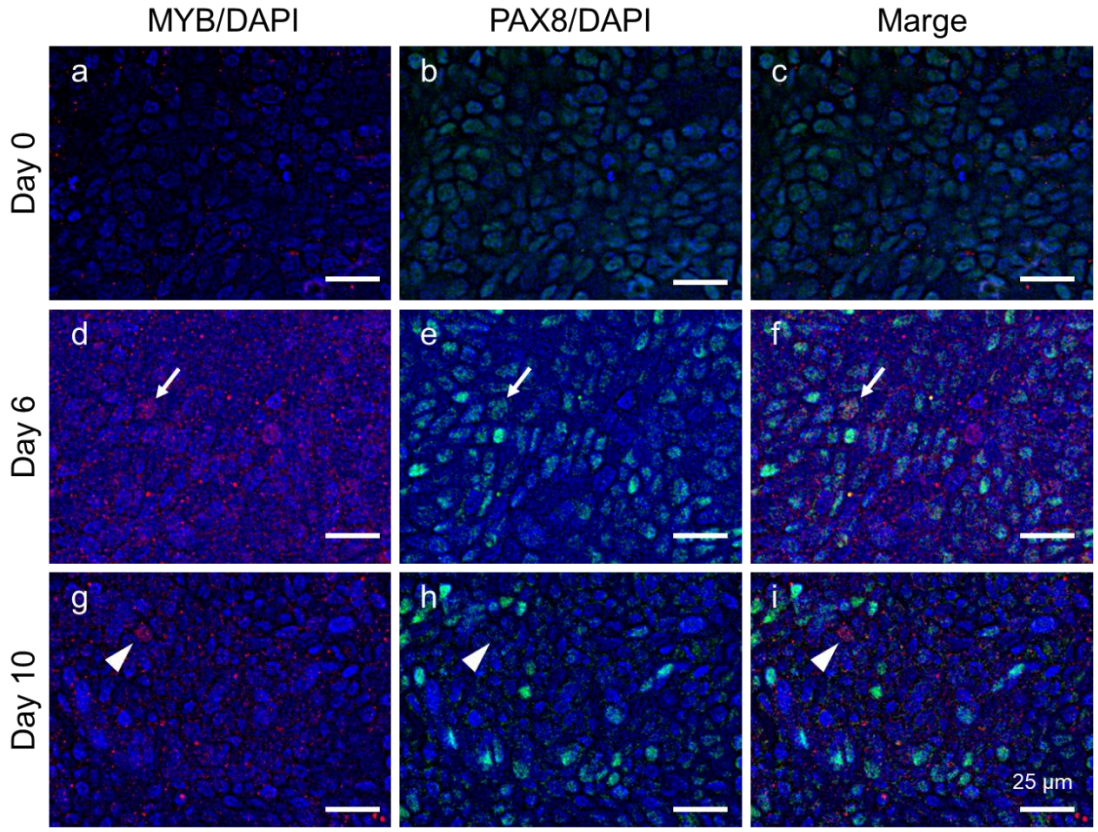
MYB/DAPI
PAX8/DAPI
Marge
Day 0
Day 6
Day 10
a
b
c
d
e
f
g
h
i
25 μm

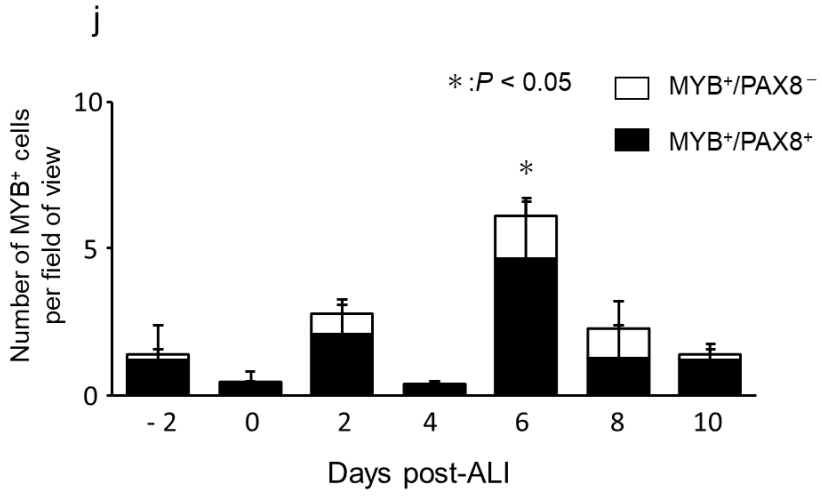
j
＊:P < 0.05
MYB+/PAX8−
MYB+/PAX8+
Number of MYB+ cells per field of view
10
5
0
＊
- 2
0
2
4
6
8
10
Days post-ALI

Fig. 15

Co-localization of MYB and PAX8 in ALI cultured bovine oviductal epithelial cells (**a-i**). Distributions of cells showing positive staining for MYB (red) and PAX8 (green) in the ALI cultured bovine oviductal epithelial cells. Arrows indicate the cells that were double-positive for MYB and PAX8, and arrowheads indicate the cells that were positive for MYB and negative for PAX8. Cell nuclei were counter-stained with DAPI (blue). Scale bars represent 25 μm. (**j**) Change in the number (mean ± SEM, n = 7) of MYB^+ cells per field of view. The black bars indicate the number of cells that were double-positive for MYB and PAX8, and the white bars indicate the number of cells that were positive for MYB and negative for PAX8. The asterisk indicates $P < 0.05$ when compared to before the onset of ALI (Days -2).

DISCUSSION

Cyclic morphological changes occur during the estrous cycle in the oviductal epithelium, and these changes provide a suitable micro-environment for gamete transport, fertilization, and early embryonic development [32,34]. However, the mechanisms of the cyclic changes that occur within the bovine oviduct have remained unclear. In the chapter 3, we have investigated ciliogenesis process in the bovine oviductal epithelial cells based on the immunohistochemical classification. In this chapter, we attempted to further explore multi-step process of ciliogenesis in the bovine oviductal epithelial cells by means of ALI culture system.

The culture models are useful tools for revealing physiology and biochemistry of cells, and various cell culture models for primary bovine oviductal epithelial cells were established to study physiological events [92,104]. To understand oviductal physiology and ciliogenesis, *in vitro* models that can induce ciliogenesis are needed.

ALI culture system is widely adopted for studying ciliogenesis process in the airway epithelial cells, since epithelial cells cultured at the ALI become better differentiated and polarized [62,112]. Similar to airway epithelial cells, oviductal epithelial cells also undergo ciliogenesis with the ALI culture condition [32,111]. Thus, in the present study, we examined the temporal ciliogenesis in the ALI cultured bovine oviductal epithelial cells and compared it with *in vivo* condition.

High proliferative activity of cultured epithelial cells was observed at day 0, and from then onwards cells underwent limited proliferation (Fig. 12n). Ciliogenesis characterized by the increase in the number of acetylated-α-tubulin^{+} cells was observed at day 2 (Fig. 12o). Given that ciliogenesis occurs in the non-proliferating cells [85,86],

it is possible that post-proliferating cells undergo ciliogenesis in the cultured epithelial cells.

In ALI cultures of airway epithelial cells, a steady increase of the FOXJ1 mRNA expression has been observed for up to day 14 post-ALI [107,112]. On the other hand, as shown in Fig. 13, the FOXJ1 mRNA expression continued to increase up to day 4, and then its expression decreased over the ALI culture period (Fig. 13). In association with the decrease of the FOXJ1 mRNA expression, the number of $FOXJ1^{+}$ cells also continued to decrease from day 4 to day 10 (Fig. 14k). In addition, double positive and negative for FOXJ1 and PAX8 cells which were absent in the bovine oviductal epithelium were present in the ALI cultured of bovine oviductal epithelial cells (Fig. 14a-c). The number of $FOXJ1^{-}/PAX8^{-}$ cells gradually increased from day 6 to day 10 (Fig. 14l). These observations implied that our ALI culture system is not sufficient to induce ciliogenesis in the bovine oviductal epithelial cells. It is reported that long time cultured bovine epithelial cells show elongated morphology, and lose the epithelial characteristics [106,113]. In the present study, since epithelial cells were cultured for 14 days after seeding, it is possible that cells acquired non-epithelial characteristics, resulting in the appearance of the $FOXJ1^{-}/PAX8^{-}$ or $FOXJ1^{+}/PAX8^{+}$ cells in the ALI cultured cells. Therefore, our ALI culture system may not adequately mimic the *in vivo* microenvironment. To obtain valid information, further experiment using better culture system will be needed.

In our ALI culture, the results showed the existence of MYB+ epithelial cells as well as *in vivo* condition (Fig. 15a-i). MYB is involved in centriole amplification during ciliogenesis [62], and is able to induce FOXJ1 expression in the mouse airway epithelial cells. However, the number of $FOXJ1^{+}$ cells reached at maximum at day 4, and that of

MYB^+ cells became highest at day 6 during the ALI culture (Fig. 15j). These expression patterns of MYB and FOXJ1 were completely different from the *in vivo* situation. Moreover, in the bovine oviductal epithelial tissue, most of MYB^+ cells were positive for FOXJ1 (Fig. 8j), while most of MYB^+ cells were positive for PAX8 in the ALI cultured epithelial cells (Fig. 15a-i). Given that MYB is able to induce FOXJ1 expression, it is possible that $PAX8^+/MYB^+$ cells failed to induce FOXJ1 expression. Ciliogenesis is a multistep process tightly controlled with several ciliogenesis associated factors. Palma-Vera et al. (2014) reported that bovine oviductal epithelial cells cultured by ALI in the media without any supplement factors could not undergo ciliogenesis *in vitro* although they established apical-basolateral polarity [114]. Thus, not only exposure apical to air but also use certain factors regulating ciliogenesis may necessary for induction of ciliogenesis in cultured cells. To mimic *in vivo* ciliogenesis using *in vitro* cell culture it will be important to elucidate regulation mechanisms of ciliogenesis related factors in the bovine oviduct.

Several studies have suggested that E2 plays a role in the ciliogenesis in the oviduct [66,115]. The highest number of ciliated cells in the bovine oviduct was observed at around the time of ovulation when the oviductal tissue concentration of E2 is the highest (see chapter 3, Fig. 6e). These observations provided the possibility that lack of E2 signaling resulted in the failure of ciliogenesis in the present study. In addition, the necessity of interaction between epithelial cells and stromal cells in induction of ciliogenesis is reported. Nakao et al. (2017) found that oviductal extracellular vesicles derived from mesenchymal cells promoted ciliogenesis in the mouse oviduct [116]. Other studies have suggested that oviductal mesenchyme cells determined the fate of epithelial cells [117]. Therefore, some factors derived from stromal cells may be also necessary for

the ciliogenesis in the ALI cultured bovine oviductal epithelial cells. Co-culture of epithelial cells with stromal cells might promote formation of cilia in the cultured cells.

In summary, our results showed that ciliogenesis in the bovine oviductal epithelial cells during the ALI culture was different from the *in vivo* ciliogenesis. Our findings implied that ciliogenesis trigged by the ALI culture in the bovine oviductal epithelial cells does not precisely imitate *in vivo* ciliogenesis. To reveal ciliogenesis process of the bovine oviductal epithelial cells, establishment of adequate culture system that could be evaluate the ciliogenesis will be need.

SUMMARY

Oviductal epithelium consists ciliated and non-ciliated cells. Our previous study suggested that the oviductal epithelium contains at least seven types of cells in terms of immunological classification, and they might be at different stages of ciliogenesis. However, precise ciliogenesis mechanism in the bovine oviductal epithelial cells remains unclear. In this chapter, to clarify the ciliogenesis process in the bovine oviductal epithelial cells, temporal ciliogenesis in the cells cultured by the air-liquid interface (ALI), which can induce ciliogenesis *in vitro*, was compared with *in vivo* condition. We examined the expression of FOXJ1 and MYB (ciliogenesis markers), and PAX8 (non-ciliated cell marker) in the bovine oviductal epithelial cells cultured by ALI at two-day intervals over a period of 10 days from the onset of ALI to clarify detailed temporal ciliogenesis. Proliferation and ciliogenesis of the bovine oviductal epithelial cells were assessed using immunostaining of Ki67 and acetylated-α-tubulin, respectively. Followed by the high proliferative activity at day 0 of ALI culture, ciliogenesis was observed at day 2. However, the FOXJ1 and MYB mRNA expression continued to decrease from day 4 and day 6 to day 10, respectively. Consistent with the decrease of gene expression of FOXJ1 and MYB, the numbers of $FOXJ1^+$ and MYB^+ cells decreased over the course of ALI culture. We identified double positive and negative for both FOXJ1 and PAX8 in the ALI cultured epithelial cells which were never found in *in vivo* condition. In conclusion, our results showed that ciliogenesis in the bovine oviductal epithelial cells during the ALI culture was different from the *in vivo* condition. To reveal ciliogenesis process of the bovine oviductal epithelial cells precisely, establishment of adequate culture system in which the ciliogenesis could be evaluate will be need.

CHAPTER 5
CONCLUSIONS

The present study investigated that the mechanisms of the changes in the number of ciliated and non-ciliated cells in the bovine oviductal epithelium during the estrous cycle. The first series of experiments showed that the oviductal epithelium was remodeled, and the proportions of ciliated and non-ciliated cells in the bovine oviductal epithelium was regulated by proliferation and apoptosis during the estrous cycle. The second series of experiments implied that based on immunological classification, at least seven types of cells were present in the bovine oviductal epithelium, and they might be at different stages of ciliogenesis. In the third series of experiments, ciliogenesis in the bovine oviductal epithelial cells cultured at the ALI was different from the *in vivo* condition due to poor culture condition. Thus, to reveal ciliogenesis process of the bovine oviductal epithelial cells precisely, establishment of adequate culture system will be need.

Overall results suggested that cell proliferation, apoptosis, and ciliogenesis contributed to changing in the composition of oviductal epithelium during the estrous cycle. These cyclic morphological changes provide the optimal environment for gamete transport, fertilization and embryo development within the oviduct.

REFERENCES

1. Menezo Y, Guerin P (1997) The mammalian oviduct: biochemistry and physiology. Eur J Obstet Gynecol Reprod Biol 73 (1):99-104

2. Croxatto HB (2002) Physiology of gamete and embryo transport through the fallopian tube. Reprod Biomed Online 4 (2):160-169

3. Halbert SA, Tam PY, Blandau RJ (1976) Egg transport in the rabbit oviduct: the roles of cilia and muscle. Science 191 (4231):1052-1053. doi:10.1126/science.1251215

4. Hunter RH (1998) Have the Fallopian tubes a vital rôle in promoting fertility? Acta Obstet Gynecol Scand 77 (5):475-486

5. Hunter RH (2012) Components of oviduct physiology in eutherian mammals. Biol Rev Camb Philos Soc 87 (1):244-255. doi:10.1111/j.1469-185X.2011.00196.x

6. Suarez SS, Brockman K, Lefebvre R (1997) Distribution of mucus and sperm in bovine oviducts after artificial insemination: the physical environment of the oviductal sperm reservoir. Biol Reprod 56 (2):447-453. doi:10.1095/biolreprod56.2.447

7. Pulkkinen MO (1995) Oviductal function is critical for very early human life. Ann Med 27 (3):307-310. doi:10.3109/07853899509002582

8. Jeoung M, Lee S, Hawng HK, Cheon YP, Jeong YK, Gye MC, Iglarz M, Ko C, Bridges PJ (2010) Identification of a novel role for endothelins within the oviduct. Endocrinology 151 (6):2858-2867. doi:10.1210/en.2009-1155

9. Afzelius BA (2004) Cilia-related diseases. J Pathol 204 (4):470-477. doi:10.1002/path.1652

10. Yoshimoto Y, Nishie T, Ito S, Kobayashi Y, Yamamoto Y, Okuda K, Kimura K (2017) Adrenomedullin regulates the speed of oviductal fluid flow in cattle. Mol Reprod Dev 84 (8):712-718. doi:10.1002/mrd.22852

11. Verdugo P, Rumery RE, Tam PY (1980) Hormonal control of oviductal ciliary activity: effect of prostaglandins. Fertil Steril 33 (2):193-196. doi:10.1016/s0015-0282(16)44541-3

12. Hermoso M, Barrera N, Morales B, Pérez S, Villalón M (2001) Platelet activating factor increases ciliary activity in the hamster oviduct through epithelial production of prostaglandin E2. Pflugers Arch 442 (3):336-345. doi:10.1007/s004240100550

13. Liao SB, Cheung KH, Cheung MP, To YT, O WS, Tang F (2013) Adrenomedullin increased the short-circuit current in the pig oviduct through chloride channels via the CGRP receptor: mediation by cAMP and calcium ions but not by nitric oxide. Biol Reprod 89 (4):99. doi:10.1095/biolreprod.113.109934

14. Paltieli Y, Eibschitz I, Ziskind G, Ohel G, Silbermann M, Weichselbaum A (2000) High progesterone levels and ciliary dysfunction--a possible cause of ectopic pregnancy.

J Assist Reprod Genet 17 (2):103-106. doi:10.1023/a:1009465900824
15. Papathanasiou A, Djahanbakhch O, Saridogan E, Lyons RA (2008) The effect of interleukin-6 on ciliary beat frequency in the human fallopian tube. Fertil Steril 90 (2):391-394. doi:10.1016/j.fertnstert.2007.07.1379
16. Liao SB, Li HW, Ho JC, Yeung WS, Ng EH, Cheung AN, Tang F, O WS (2012) Possible role of adrenomedullin in the pathogenesis of tubal ectopic pregnancy. J Clin Endocrinol Metab 97 (6):2105-2112. doi:10.1210/jc.2011-3290
17. Vasquez G, Winston RM, Brosens IA (1983) Tubal mucosa and ectopic pregnancy. Br J Obstet Gynaecol 90 (5):468-474. doi:10.1111/j.1471-0528.1983.tb08946.x
18. Shaw JL, Dey SK, Critchley HO, Horne AW (2010) Current knowledge of the aetiology of human tubal ectopic pregnancy. Hum Reprod Update 16 (4):432-444. doi:10.1093/humupd/dmp057
19. Walker JJ (2007) Ectopic pregnancy. Clin Obstet Gynecol 50 (1):89-99. doi:10.1097/GRF.0b013e31802f4f79
20. Farquhar CM (2005) Ectopic pregnancy. Lancet 366 (9485):583-591. doi:10.1016/S0140-6736(05)67103-6
21. Varma R, Gupta J (2009) Tubal ectopic pregnancy. BMJ Clin Evid 2009
22. Waylen AL, Metwally M, Jones GL, Wilkinson AJ, Ledger WL (2009) Effects of cigarette smoking upon clinical outcomes of assisted reproduction: a meta-analysis. Hum Reprod Update 15 (1):31-44. doi:10.1093/humupd/dmn046
23. Wang X, Lee CL, Li RHW, Vijayan M, Duan YG, Yeung WSB, Zhang Y, Chiu PCN (2019) Alteration of the immune cell profiles in the pathophysiology of tubal ectopic pregnancy. Am J Reprod Immunol 81 (4):e13093. doi:10.1111/aji.13093
24. Praveen K, Davis EE, Katsanis N (2015) Unique among ciliopathies: primary ciliary dyskinesia, a motile cilia disorder. F1000Prime Rep 7:36. doi:10.12703/P7-36
25. Smith LJ, West N, Hughes D, Marshall H, Johns CS, Stewart NJ, Chan HF, Rao M, Capener DJ, Bray J, Collier GJ, Hughes PJC, Norquay G, Schofield L, Chetcuti P, Moya E, Wild JM (2018) Imaging Lung Function Abnormalities in Primary Ciliary Dyskinesia Using Hyperpolarized Gas Ventilation MRI. Ann Am Thorac Soc 15 (12):1487-1490. doi:10.1513/AnnalsATS.201711-890RL
26. Spassky N, Meunier A (2017) The development and functions of multiciliated epithelia. Nat Rev Mol Cell Biol 18 (7):423-436. doi:10.1038/nrm.2017.21
27. Wanner A, Salathé M, O'Riordan TG (1996) Mucociliary clearance in the airways. Am J Respir Crit Care Med 154 (6 Pt 1):1868-1902. doi:10.1164/ajrccm.154.6.8970383
28. Sawamoto K, Wichterle H, Gonzalez-Perez O, Cholfin JA, Yamada M, Spassky N, Murcia NS, Garcia-Verdugo JM, Marin O, Rubenstein JL, Tessier-Lavigne M, Okano H,

Alvarez-Buylla A (2006) New neurons follow the flow of cerebrospinal fluid in the adult brain. Science 311 (5761):629-632. doi:10.1126/science.1119133
29. Lyons RA, Saridogan E, Djahanbakhch O (2006) The reproductive significance of human Fallopian tube cilia. Hum Reprod Update 12 (4):363-372. doi:10.1093/humupd/dml012
30. Halbert SA, Patton DL, Zarutskie PW, Soules MR (1997) Function and structure of cilia in the fallopian tube of an infertile woman with Kartagener's syndrome. Hum Reprod 12 (1):55-58. doi:10.1093/humrep/12.1.55
31. Li S, Winuthayanon W (2017) Oviduct: roles in fertilization and early embryo development. J Endocrinol 232 (1):R1-R26. doi:10.1530/JOE-16-0302
32. Chen S, Einspanier R, Schoen J (2013) In vitro mimicking of estrous cycle stages in porcine oviduct epithelium cells: estradiol and progesterone regulate differentiation, gene expression, and cellular function. Biol Reprod 89 (3):54. doi:10.1095/biolreprod.113.108829
33. Abe H, Hoshi H (2007) Regional and cyclic variations in the ultrastructural features of secretory cells in the oviductal epithelium of the Chinese Meishan pig. Reprod Domest Anim 42 (3):292-298. doi:10.1111/j.1439-0531.2006.00781.x
34. Abe H, Oikawa T (1993) Observations by scanning electron microscopy of oviductal epithelial cells from cows at follicular and luteal phases. Anat Rec 235 (3):399-410. doi:10.1002/ar.1092350309
35. Freeman DA, Weber JA, Geary RT, Woods GL (1991) Time of embryo transport through the mare oviduct. Theriogenology 36 (5):823-830. doi:10.1016/0093-691x(91)90348-h
36. Okuda K, Kito S, Sumi N, Sato K (1988) A study of the central cavity in the bovine corpus luteum. Vet Rec 123 (7):180-183. doi:10.1136/vr.123.7.180
37. Miyamoto Y, Skarzynski DJ, Okuda K (2000) Is tumor necrosis factor alpha a trigger for the initiation of endometrial prostaglandin F(2alpha) release at luteolysis in cattle? Biol Reprod 62 (5):1109-1115. doi:10.1095/biolreprod62.5.1109
38. Arai M, Yoshioka S, Tasaki Y, Okuda K (2013) Remodeling of bovine endometrium throughout the estrous cycle. Anim Reprod Sci 142 (1-2):1-9. doi:10.1016/j.anireprosci.2013.08.003
39. Hojo T, Al-Zi'abi MO, Skarzynski DJ, Acosta TJ, Okuda K (2009) Changes in the vasculature of bovine corpus luteum during the estrous cycle and prostaglandin F2alpha-induced luteolysis. J Reprod Dev 55 (5):512-517. doi:10.1262/jrd.20257
40. Blanpain C, Horsley V, Fuchs E (2007) Epithelial stem cells: turning over new leaves. Cell 128 (3):445-458. doi:10.1016/j.cell.2007.01.014

41. Di Bernardo J, Maiden MM, Hershenson MB, Kunisaki SM (2014) Amniotic fluid derived mesenchymal stromal cells augment fetal lung growth in a nitrofen explant model. J Pediatr Surg 49 (6):859-864; discussion 864-855. doi:10.1016/j.jpedsurg.2014.01.013
42. Bowden DH (1983) Cell turnover in the lung. Am Rev Respir Dis 128 (2 Pt 2):S46-48. doi:10.1164/arrd.1983.128.2P2.S46
43. Steffl M, Schweiger M, Amselgruber WM (2004) Immunophenotype of porcine oviduct epithelial cells during the oestrous cycle: a double-labelling immunohistochemical study. Histochem Cell Biol 121 (3):239-244. doi:10.1007/s00418-004-0632-x
44. Steinhauer N, Boos A, Günzel-Apel AR (2004) Morphological changes and proliferative activity in the oviductal epithelium during hormonally defined stages of the oestrous cycle in the bitch. Reprod Domest Anim 39 (2):110-119. doi:10.1111/j.1439-0531.2004.00490.x
45. Desantis S, Zizza S, Accogli G, Acone F, Rossi R, Resta L (2011) Morphometric and ultrastructural features of the mare oviduct epithelium during oestrus. Theriogenology 75 (4):671-678. doi:10.1016/j.theriogenology.2010.10.007
46. Donnez J, Casanas-Roux F, Caprasse J, Ferin J, Thomas K (1985) Cyclic changes in ciliation, cell height, and mitotic activity in human tubal epithelium during reproductive life. Fertil Steril 43 (4):554-559. doi:10.1016/s0015-0282(16)48496-7
47. Wijayagunawardane MP, Miyamoto A, Cerbito WA, Acosta TJ, Takagi M, Sato K (1998) Local distributions of oviductal estradiol, progesterone, prostaglandins, oxytocin and endothelin-1 in the cyclic cow. Theriogenology 49 (3):607-618
48. Hansen TR, Randel RD, Welsh TH (1988) Granulosa cell steroidogenesis and follicular fluid steroid concentrations after the onset of oestrus in cows. J Reprod Fertil 84 (2):409-416. doi:10.1530/jrf.0.0840409
49. Jabbour HN, Kelly RW, Fraser HM, Critchley HO (2006) Endocrine regulation of menstruation. Endocr Rev 27 (1):17-46. doi:10.1210/er.2004-0021
50. Harada T, Kaponis A, Iwabe T, Taniguchi F, Makrydimas G, Sofikitis N, Paschopoulos M, Paraskevaidis E, Terakawa N (2004) Apoptosis in human endometrium and endometriosis. Hum Reprod Update 10 (1):29-38. doi:10.1093/humupd/dmh007
51. Appino S, Vincenti L, Rota A, Pellegrini S, Chieppa MN, Cadoni V, Pregel P (2015) Chlamydia abortus in Cows Oviducts, Occasional Event or Causal Connection? Reprod Domest Anim 50 (3):526-528. doi:10.1111/rda.12505
52. Jin Z, El-Deiry WS (2005) Overview of cell death signaling pathways. Cancer Biol Ther 4 (2):139-163. doi:10.4161/cbt.4.2.1508
53. Pellettieri J, Sánchez Alvarado A (2007) Cell turnover and adult tissue homeostasis:

from humans to planarians. Annu Rev Genet 41:83-105. doi:10.1146/annurev.genet.41.110306.130244
54. Katoh H, Fujita Y (2012) Epithelial homeostasis: elimination by live cell extrusion. Curr Biol 22 (11):R453-455. doi:10.1016/j.cub.2012.04.036
55. Pier B, Kazanjian A, Gillette L, Strenge K, Burney RO (2013) Effect of cigarette smoking on human oviductal ciliation and ciliogenesis. Fertil Steril 99 (1):199-205. doi:10.1016/j.fertnstert.2012.08.041
56. Lau A, Kollara A, St John E, Tone AA, Virtanen C, Greenblatt EM, King WA, Brown TJ (2014) Altered expression of inflammation-associated genes in oviductal cells following follicular fluid exposure: implications for ovarian carcinogenesis. Exp Biol Med (Maywood) 239 (1):24-32. doi:10.1177/1535370213508216
57. Pardo-Saganta A, Law BM, Tata PR, Villoria J, Saez B, Mou H, Zhao R, Rajagopal J (2015) Injury induces direct lineage segregation of functionally distinct airway basal stem/progenitor cell subpopulations. Cell Stem Cell 16 (2):184-197. doi:10.1016/j.stem.2015.01.002
58. Jain R, Ray JM, Pan JH, Brody SL (2012) Sex hormone-dependent regulation of cilia beat frequency in airway epithelium. Am J Respir Cell Mol Biol 46 (4):446-453. doi:10.1165/rcmb.2011-0107OC
59. Chu DT, Klymkowsky MW (1989) The appearance of acetylated alpha-tubulin during early development and cellular differentiation in Xenopus. Dev Biol 136 (1):104-117
60. Bowen NJ, Logani S, Dickerson EB, Kapa LB, Akhtar M, Benigno BB, McDonald JF (2007) Emerging roles for PAX8 in ovarian cancer and endosalpingeal development. Gynecol Oncol 104 (2):331-337. doi:10.1016/j.ygyno.2006.08.052
61. Akison LK, Boden MJ, Kennaway DJ, Russell DL, Robker RL (2014) Progesterone receptor-dependent regulation of genes in the oviducts of female mice. Physiol Genomics 46 (16):583-592. doi:10.1152/physiolgenomics.00044.2014
62. Tan FE, Vladar EK, Ma L, Fuentealba LC, Hoh R, Espinoza FH, Axelrod JD, Alvarez-Buylla A, Stearns T, Kintner C, Krasnow MA (2013) Myb promotes centriole amplification and later steps of the multiciliogenesis program. Development 140 (20):4277-4286. doi:10.1242/dev.094102
63. Yu X, Ng CP, Habacher H, Roy S (2008) Foxj1 transcription factors are master regulators of the motile ciliogenic program. Nat Genet 40 (12):1445-1453. doi:10.1038/ng.263
64. Scholzen T, Gerdes J (2000) The Ki-67 protein: from the known and the unknown. J Cell Physiol 182 (3):311-322. doi:10.1002/(SICI)1097-4652(200003)182:3<311::AID-JCP1>3.0.CO;2-9

65. Ito S, Kobayashi Y, Yamamoto Y, Kimura K, Okuda K (2016) Remodeling of bovine oviductal epithelium by mitosis of secretory cells. Cell Tissue Res 366 (2):403-410. doi:10.1007/s00441-016-2432-8
66. Anderson RG, Brenner RM (1971) The formation of basal bodies (centrioles) in the Rhesus monkey oviduct. J Cell Biol 50 (1):10-34
67. Sorokin SP (1968) Reconstructions of centriole formation and ciliogenesis in mammalian lungs. J Cell Sci 3 (2):207-230
68. Rock JR, Hogan BL (2011) Epithelial progenitor cells in lung development, maintenance, repair, and disease. Annu Rev Cell Dev Biol 27:493-512. doi:10.1146/annurev-cellbio-100109-104040
69. Rawlins EL, Hogan BL (2008) Ciliated epithelial cell lifespan in the mouse trachea and lung. Am J Physiol Lung Cell Mol Physiol 295 (1):L231-234. doi:10.1152/ajplung.90209.2008
70. Chen F, Fine A (2016) Stem Cells in Lung Injury and Repair. Am J Pathol 186 (10):2544-2550. doi:10.1016/j.ajpath.2016.05.023
71. Rock JR, Onaitis MW, Rawlins EL, Lu Y, Clark CP, Xue Y, Randell SH, Hogan BL (2009) Basal cells as stem cells of the mouse trachea and human airway epithelium. Proc Natl Acad Sci U S A 106 (31):12771-12775. doi:10.1073/pnas.0906850106
72. Rawlins EL, Okubo T, Xue Y, Brass DM, Auten RL, Hasegawa H, Wang F, Hogan BL (2009) The role of Scgb1a1+ Clara cells in the long-term maintenance and repair of lung airway, but not alveolar, epithelium. Cell Stem Cell 4 (6):525-534. doi:10.1016/j.stem.2009.04.002
73. Song H, Yao E, Lin C, Gacayan R, Chen MH, Chuang PT (2012) Functional characterization of pulmonary neuroendocrine cells in lung development, injury, and tumorigenesis. Proc Natl Acad Sci U S A 109 (43):17531-17536. doi:10.1073/pnas.1207238109
74. Ireland JJ, Murphee RL, Coulson PB (1980) Accuracy of predicting stages of bovine estrous cycle by gross appearance of the corpus luteum. J Dairy Sci 63 (1):155-160. doi:10.3168/jds.S0022-0302(80)82901-8
75. Meunier A, Azimzadeh J (2016) Multiciliated Cells in Animals. Cold Spring Harb Perspect Biol 8 (12). doi:10.1101/cshperspect.a028233
76. Jackson PK, Attardi LD (2016) p73 and FoxJ1: Programming Multiciliated Epithelia. Trends Cell Biol 26 (4):239-240. doi:10.1016/j.tcb.2016.03.001
77. You Y, Huang T, Richer EJ, Schmidt JE, Zabner J, Borok Z, Brody SL (2004) Role of f-box factor foxj1 in differentiation of ciliated airway epithelial cells. Am J Physiol Lung Cell Mol Physiol 286 (4):L650-657. doi:10.1152/ajplung.00170.2003

78. Li S, O'Neill SR, Zhang Y, Holtzman MJ, Takemaru KI, Korach KS, Winuthayanon W (2017) Estrogen receptor α is required for oviductal transport of embryos. FASEB J 31 (4):1595-1607. doi:10.1096/fj.201601128R
79. Pardo-Saganta A, Law BM, Gonzalez-Celeiro M, Vinarsky V, Rajagopal J (2013) Ciliated cells of pseudostratified airway epithelium do not become mucous cells after ovalbumin challenge. Am J Respir Cell Mol Biol 48 (3):364-373. doi:10.1165/rcmb.2012-0146OC
80. Pan JH, Adair-Kirk TL, Patel AC, Huang T, Yozamp NS, Xu J, Reddy EP, Byers DE, Pierce RA, Holtzman MJ, Brody SL (2014) Myb permits multilineage airway epithelial cell differentiation. Stem Cells 32 (12):3245-3256. doi:10.1002/stem.1814
81. Wang L, Fu C, Fan H, Du T, Dong M, Chen Y, Jin Y, Zhou Y, Deng M, Gu A, Jing Q, Liu T (2013) miR-34b regulates multiciliogenesis during organ formation in zebrafish. Development 140 (13):2755-2764. doi:10.1242/dev.092825
82. Look DC, Walter MJ, Williamson MR, Pang L, You Y, Sreshta JN, Johnson JE, Zander DS, Brody SL (2001) Effects of paramyxoviral infection on airway epithelial cell Foxj1 expression, ciliogenesis, and mucociliary function. Am J Pathol 159 (6):2055-2069. doi:10.1016/S0002-9440(10)63057-X
83. Hsu HS, Liu CC, Lin JH, Hsu TW, Su K, Hung SC (2014) Repair of naphthalene-induced acute tracheal injury by basal cells depends on β-catenin. J Thorac Cardiovasc Surg 148 (1):322-332. doi:10.1016/j.jtcvs.2013.10.039
84. Vladar EK, Stratton MB, Saal ML, Salazar-De Simone G, Wang X, Wolgemuth D, Stearns T, Axelrod JD (2018) Cyclin-dependent kinase control of motile ciliogenesis. Elife 7. doi:10.7554/eLife.36375
85. Otto T, Candido SV, Pilarz MS, Sicinska E, Bronson RT, Bowden M, Lachowicz IA, Mulry K, Fassl A, Han RC, Jecrois ES, Sicinski P (2017) Cell cycle-targeting microRNAs promote differentiation by enforcing cell-cycle exit. Proc Natl Acad Sci U S A 114 (40):10660-10665. doi:10.1073/pnas.1702914114
86. Park KS, Wells JM, Zorn AM, Wert SE, Laubach VE, Fernandez LG, Whitsett JA (2006) Transdifferentiation of ciliated cells during repair of the respiratory epithelium. Am J Respir Cell Mol Biol 34 (2):151-157. doi:10.1165/rcmb.2005-0332OC
87. Erjefält JS, Erjefält I, Sundler F, Persson CG (1995) In vivo restitution of airway epithelium. Cell Tissue Res 281 (2):305-316. doi:10.1007/bf00583399
88. Tadokoro T, Wang Y, Barak LS, Bai Y, Randell SH, Hogan BL (2014) IL-6/STAT3 promotes regeneration of airway ciliated cells from basal stem cells. Proc Natl Acad Sci U S A 111 (35):E3641-3649. doi:10.1073/pnas.1409781111
89. Schmid A, Sailland J, Novak L, Baumlin N, Fregien N, Salathe M (2017) Modulation

of Wnt signaling is essential for the differentiation of ciliated epithelial cells in human airways. FEBS Lett 591 (21):3493-3506. doi:10.1002/1873-3468.12851
90. Ghosh A, Syed SM, Tanwar PS (2017) genetic cell lineage tracing reveals that oviductal secretory cells self-renew and give rise to ciliated cells. Development 144 (17):3031-3041. doi:10.1242/dev.149989
91. Tríbulo P, Siqueira LGB, Oliveira LJ, Scheffler T, Hansen PJ (2018) Identification of potential embryokines in the bovine reproductive tract. J Dairy Sci 101 (1):690-704. doi:10.3168/jds.2017-13221
92. Abe H, Hoshi H (1997) Bovine oviductal epithelial cells: their cell culture and applications in studies for reproductive biology. Cytotechnology 23 (1-3):171-183. doi:10.1023/A:1007929826186
93. Bongso A, Ng SC, Sathananthan H, Ng PL, Rauff M, Ratnam SS (1989) Establishment of human ampullary cell cultures. Hum Reprod 4 (5):486-494. doi:10.1093/oxfordjournals.humrep.a136932
94. Bouliant A, Greig AS, Genest P (1973) Biological characterization of a cell line derived from the pig oviduct. In Vitro 9 (2):92-102. doi:10.1007/bf02616006
95. Ouhibi N, Menezo Y, Benet G, Nicollet B (1989) Culture of epithelial cells derived from the oviduct of different species. Hum Reprod 4 (3):229-235. doi:10.1093/oxfordjournals.humrep.a136877
96. Takeuchi K, Maruyama I, Yamamoto S, Oki T, Nagata Y (1991) Isolation and monolayer culture of human fallopian tube epithelial cells. In Vitro Cell Dev Biol 27A (9):720-724. doi:10.1007/bf02633217
97. Rottmayer R, Ulbrich SE, Kölle S, Prelle K, Neumueller C, Sinowatz F, Meyer HH, Wolf E, Hiendleder S (2006) A bovine oviduct epithelial cell suspension culture system suitable for studying embryo-maternal interactions: morphological and functional characterization. Reproduction 132 (4):637-648. doi:10.1530/rep.1.01136
98. Reischl J, Prelle K, Schöl H, Neumüller C, Einspanier R, Sinowatz F, Wolf E (1999) Factors affecting proliferation and dedifferentiation of primary bovine oviduct epithelial cells in vitro. Cell Tissue Res 296 (2):371-383. doi:10.1007/s004410051297
99. Coleman DL, Tuet IK, Widdicombe JH (1984) Electrical properties of dog tracheal epithelial cells grown in monolayer culture. Am J Physiol 246 (3 Pt 1):C355-359. doi:10.1152/ajpcell.1984.246.3.C355
100. Macdonald NP, Zhu F, Hall CJ, Reboud J, Crosier PS, Patton EE, Wlodkowic D, Cooper JM (2016) Assessment of biocompatibility of 3D printed photopolymers using zebrafish embryo toxicity assays. Lab Chip 16 (2):291-297. doi:10.1039/c5lc01374g
101. Pruniéras M, Régnier M, Woodley D (1983) Methods for cultivation of keratinocytes

with an air-liquid interface. J Invest Dermatol 81 (1 Suppl):28s-33s. doi:10.1111/1523-1747.ep12540324
102. Whitcutt MJ, Adler KB, Wu R (1988) A biphasic chamber system for maintaining polarity of differentiation of cultured respiratory tract epithelial cells. In Vitro Cell Dev Biol 24 (5):420-428. doi:10.1007/bf02628493
103. Ong HX, Jackson CL, Cole JL, Lackie PM, Traini D, Young PM, Lucas J, Conway J (2016) Primary Air-Liquid Interface Culture of Nasal Epithelium for Nasal Drug Delivery. Mol Pharm 13 (7):2242-2252. doi:10.1021/acs.molpharmaceut.5b00852
104. Ferraz MAMM, Henning HHW, Stout TAE, Vos PLAM, Gadella BM (2017) Designing 3-Dimensional In Vitro Oviduct Culture Systems to Study Mammalian Fertilization and Embryo Production. Ann Biomed Eng 45 (7):1731-1744. doi:10.1007/s10439-016-1760-x
105. Fotheringham S, Levanon K, Drapkin R (2011) Ex vivo culture of primary human fallopian tube epithelial cells. J Vis Exp (51). doi:10.3791/2728
106. Gualtieri R, Mollo V, Braun S, Barbato V, Fiorentino I, Talevi R (2012) Long-term viability and differentiation of bovine oviductal monolayers: bidimensional versus three-dimensional culture. Theriogenology 78 (7):1456-1464. doi:10.1016/j.theriogenology.2012.06.010
107. Gerovac BJ, Valencia M, Baumlin N, Salathe M, Conner GE, Fregien NL (2014) Submersion and hypoxia inhibit ciliated cell differentiation in a notch-dependent manner. Am J Respir Cell Mol Biol 51 (4):516-525. doi:10.1165/rcmb.2013-0237OC
108. Chen S, Schoen J (2019) Air-liquid interface cell culture: From airway epithelium to the female reproductive tract. Reprod Domest Anim 54 Suppl 3:38-45. doi:10.1111/rda.13481
109. Miessen K, Sharbati S, Einspanier R, Schoen J (2011) Modelling the porcine oviduct epithelium: a polarized in vitro system suitable for long-term cultivation. Theriogenology 76 (5):900-910. doi:10.1016/j.theriogenology.2011.04.021
110. Rajagopal M, Tollner TL, Finkbeiner WE, Cherr GN, Widdicombe JH (2006) Differentiated structure and function of primary cultures of monkey oviductal epithelium. In Vitro Cell Dev Biol Anim 42 (8-9):248-254. doi:10.1290/0602015.1
111. Chen S, Palma-Vera SE, Langhammer M, Galuska SP, Braun BC, Krause E, Lucas-Hahn A, Schoen J (2017) An air-liquid interphase approach for modeling the early embryo-maternal contact zone. Sci Rep 7:42298. doi:10.1038/srep42298
112. Cozens D, Sutherland E, Marchesi F, Taylor G, Berry CC, Davies RL (2018) Temporal differentiation of bovine airway epithelial cells grown at an air-liquid interface. Sci Rep 8 (1):14893. doi:10.1038/s41598-018-33180-w

113. Danesh Mesgaran S, Sharbati J, Einspanier R, Gabler C (2016) mRNA expression pattern of selected candidate genes differs in bovine oviductal epithelial cells in vitro compared with the in vivo state and during cell culture passages. Reprod Biol Endocrinol 14 (1):44. doi:10.1186/s12958-016-0176-7
114. Palma-Vera S, Einspanier R, Schoen J (2014) Bovine oviductal epithelial cells: long term culture characterization and impact of insulin on cell morphology. Reprod Biol 14 (3):206-212. doi:10.1016/j.repbio.2014.04.006
115. Okada A, Ohta Y, Brody SL, Watanabe H, Krust A, Chambon P, Iguchi T (2004) Role of foxj1 and estrogen receptor alpha in ciliated epithelial cell differentiation of the neonatal oviduct. J Mol Endocrinol 32 (3):615-625
116. Nakano S, Yamamoto S, Okada A, Nakajima T, Sato M, Takagi T, Tomooka Y (2017) Role of extracellular vesicles in the interaction between epithelial and mesenchymal cells during oviductal ciliogenesis. Biochem Biophys Res Commun 483 (1):245-251. doi:10.1016/j.bbrc.2016.12.158
117. Yamanouchi H, Umezu T, Tomooka Y (2010) Reconstruction of oviduct and demonstration of epithelial fate determination in mice. Biol Reprod 82 (3):528-533. doi:10.1095/biolreprod.109.078329

ABSTRACT IN JAPANESE

ウシ卵管上皮の繊毛･非繊毛細胞の増減機構の解明に関する研究

伊藤さやか

多くの哺乳動物において卵管は、受精の場であるとともに配偶子および初期胚の輸送などの様々な現象が起こる器官である。卵管はこのように、妊娠の成立において重要であるにもかかわらず、卵管の機能制御については未だ不明な点が残されている。ヒトにおいて、異所性妊娠のうち 98% は卵管でおこることや、ウシにおいても卵管機能不全による受胎率の低下が問題視されていることから、卵管機能の改善が受胎率向上に大きく寄与すると考えられる。卵管上皮は繊毛細胞ならびに非繊毛細胞の 2 種類から構成されており、繊毛細胞は細胞表面に存在する無数の繊毛を動かすことで卵管液の流れを生み出し初期胚の輸送を行う一方で、非繊毛細胞は初期胚の生存や発育に必要な物質を分泌している。このように、卵管機能は主に上皮細胞により制御される。卵管内での現象に適した微細環境を整えるために、卵管上皮細胞は発情周期に合わせて形態的･機能的に劇的な変化を起こす。卵管上皮において、繊毛細胞の割合は卵管の輸送機能が最も必要とされる排卵前後に増加し、その後黄体期には非繊毛細胞の割合が増加する。この周期的な細胞の割合の変化は卵管の機能制御において重要な役割を担うが、このメカニズムは明らかでない。本研究ではウシ卵管上皮における、繊毛･非繊毛細胞数の調節メカニズムを解明する研究の一環として、卵管上皮細胞の増殖とアポトーシスによる上皮組織の更新機構ならびに、*in vivo* および *in vitro* における非繊毛細胞から繊毛細胞への繊毛形成過程を検討した。

1. 発情周期を通じたウシ卵管上皮の更新メカニズムの解明

ウシ卵管上皮における繊毛・非繊毛細胞の割合の変化と細胞増殖および死の関連性を明らかにするために、発情周期を通じたウシ卵管膨大部ならびに峡部組織 [Day 0 (排卵日)、Days 2-3、Days 5-6、Days 8-12、Days 15-17 および Days 19-21] における Ki67 (細胞増殖マーカー)、cleaved caspase-3 (CCP3; アポトーシスマーカー) および FOXJ1 (繊毛細胞マーカー) タンパク質局在を検討し、陽性細胞率を数値化した。膨大部において Ki67 陽性細胞は発情周期を通じて確認され、Ki67 陽性細胞率は Days 19-21 で最も高く、Days 15-17 で最も低かった。峡部において、Day 0, Days 2-3, Days 5-6, Days 15-17 および Days 19-21 で Ki67 陽性細胞が観察されたが、Days 8-12 においては Ki67 陽性細胞が確認されなかった。峡部における Ki67 陽性細胞率は排卵前後に増加し、 Day 0 で最も高くなった。膨大部ならびに峡部において、発情周期を通じて CCP3 陽性細胞が観

察され、膨大部では CCP3 陽性細胞率が Days 8-12 に、峡部では Day 0 および Days 2-3 に高かった。膨大部において FOXJ1 陽性細胞率は排卵前後に有意に増加する一方、峡部における FOXJ1 陽性細胞率には有意な変化が認められなかった。続いて、細胞の増殖が繊毛細胞と非繊毛細胞のどちらで誘導されているかを明らかにするために、Ki67 と FOXJ1 ならびに PAX8 (非繊毛細胞マーカー) との共染色を行った。膨大部および峡部において、Ki67 陽性細胞は全て PAX8 陽性であり、FOXJ1 陽性細胞の中に Ki67 を発現する細胞はいなかった。以上より、排卵前には繊毛細胞の割合が増加し、その後分泌細胞の割合が増加することで、卵管内での現象に応じて卵管上皮が更新されていることが示唆された。また、卵管上皮において増殖能を有するのは非繊毛細胞のみであるにもかかわらず、繊毛細胞の割合が増加してることから、繊毛細胞は非繊毛細胞から生じる可能性が示された。

2. ウシ卵管上皮細胞における繊毛形成過程の検討

卵管と同様に繊毛・非繊毛細胞を有する気管において、非繊毛細胞が複雑な繊毛形成過程を経て繊毛細胞になることが報告されており、気管上皮には繊毛形成過程にある複数の非繊毛細胞が存在する。1. より、卵管の繊毛細胞は非繊毛細胞から生じていることを示唆する結果を得ているが、卵管の非繊毛細胞から繊毛細胞への繊毛形成過程や複数の非繊毛細胞の存在は報告されていない。そこで、ウシ卵管における繊毛形成過程を明らかにするために、ウシ卵管上皮構成細胞の詳細な解析を行った。各発情周期のウシ卵管膨大部上皮組織 (Stage I: Days 1-4, Stage II: Days 5-10, Stage III: Days 11-17, Stage IV: Days 18-20) における Ki67, Acetylated tubulin (Ac tubulin: 繊毛マーカー)、繊毛形成に必須の転写因子である FOXJ1 および MYB、PAX8（非繊毛細胞マーカー）の共局在を免疫組織化学染色法により検討し、上皮組織内腔表面 1mm あたりの細胞数の変化を調べた。全ての卵管上皮細胞は PAX8 か FOXJ1 を発現し、共発現する細胞は存在しなかったが、FOXJ1 陽性細胞中には Ac tubulin 陽性細胞と Ac tubulin 陰性細胞が存在した。よって、非繊毛細胞は PAX8 陽性細胞と FOXJ1 陽性細胞に分類されることが明らかとなった。非繊毛細胞中には MYB 陽性/PAX8 陽性または MYB 陽性/FOXJ1 陽性細胞が存在し、MYB 陽性/Ki67 陽性細胞は認められなかった。Ki67 陽性および MYB 陽性細胞数は Stage IV に増加した。以上より、卵管上皮細胞は形態学的には繊毛細胞と非繊毛細胞に大別されるが、免疫組織学的に分類すると繊毛形成過程にある少なくとも 7 段階の細胞が存在することが示唆された。また、ウシ卵管上皮の一部の非繊毛細胞は排卵に合わせて繊毛形成を完了している可能性が示された。

3. *In vitro* 培養下のウシ卵管上皮細胞における繊毛形成関連因子の発現変動

2. の結果より推測された繊毛形成経路で実際に非繊毛細胞が繊毛形成をしているか明らかにするために、培養ウシ卵管上皮細胞を用いた実験を行った。*In vitro* で繊毛形成を誘導することができる air-liquid interface (ALI) 培養法にてウシ卵管上皮細胞を培養し、2 日毎における Ki67, Ac tubulin, FOXJ1, MYB および PAX8 の発現を免疫組織化学染色法により検討し、それらの陽性細胞数を調べた。また ALI 培養細胞における繊毛形成過程を調べるために FOXJ1 および MYB mRNA 発現量を 定量的 RT-PCR により検討した。ALI 培養したウシ卵管上皮細胞において、Ac tubulin 陽性細胞数は ALI 培養開始から 2 日後 (Day 2) に最も多くなり、その後培養時間の経過につれて減少した。繊毛形成に必須の転写因子である FOXJ1 および MYB mRNA 発現量は Day 4 および Day 6 において最も高かったが、その後の発現量は共に減少した。遺伝子発現の変化と一致して、FOXJ1 陽性ならびに MYB 陽性細胞数はそれぞれ Day 4 および Day 6 に最も多かった。ALI 培養上皮細胞において、*in vivo* においては存在しない FOXJ1 陽性/PAX8 陽性および FOXJ1 陰性/PAX8 陰性細胞が認められ、FOXJ1 陰性/PAX8 陰性細胞数は培養時間と共に増加した。以上より、ALI 培養条件下で観察された繊毛形成過程は、生体内での繊毛形成過程とは全く異なっていることが明らかとなった。また、培養時間の経過につれ *in vivo* では見られない細胞が確認されたことから、今回用いた培養方法は繊毛形成過程の解明に不適切であったと考えられる。ウシ卵管上皮細胞の繊毛形成過程の全貌を明らかにするためには、*in vivo* を完全に反映する体外培養系の作出とともに更なる検討が必要である。

本研究より、卵管上皮細胞は発情周期の進行に応じて細胞増殖およびアポトーシスを起こし、卵管上皮組織を更新しており、この際に卵管上皮構成細胞が大きく変化していることが明らかとなった。卵管上皮を構成する細胞は、形態学的には繊毛細胞と非繊毛細胞の 2 種類に大別されるが、免疫組織化学的に細胞を分類すると少なくとも 7 つの細胞が存在し、これらの細胞は繊毛形成の異なる過程にある細胞であることが示唆された。また、卵管の輸送機能が最も必要とされる排卵前後の時期には、卵管の非繊毛細胞が繊毛形成を促進することで、繊毛細胞の数を増加させ、卵管の輸送機能の向上に寄与していると考えられる。このように卵管は、発情周期に合わせて卵管上皮の細胞構成を変化させることで、受精、初期胚発育や配偶子の輸送といった、卵管内で起こる様々な現象に応じた最適な環境を提供している可能性が示された。また、ALI 培養下のウシ卵管上皮細胞でみられる繊毛形成過程は *in vivo* とは異なるため、繊毛形成過程の解明には *in vivo* を正確に再現できる培養系の確立が必要である。